General Disclaimer

One or more of the Following Statements may affect this Document

- This document has been reproduced from the best copy furnished by the organizational source. It is being released in the interest of making available as much information as possible.

- This document may contain data, which exceeds the sheet parameters. It was furnished in this condition by the organizational source and is the best copy available.

- This document may contain tone-on-tone or color graphs, charts and/or pictures, which have been reproduced in black and white.

- This document is paginated as submitted by the original source.

- Portions of this document are not fully legible due to the historical nature of some of the material. However, it is the best reproduction available from the original submission.

Department of Metallurgy and Materials Science
Massachusetts Institute of Technology
Cambridge, Massachusetts

RESEARCH ON MECHANISMS OF ALLOY STRENGTHENING

I. Strengthening Through Fine Particle Dispersion

II. Control of Structure and Properties by Means of Rapid Quenching of Liquid Metals (Splat Cooling)

Semi-Annual Report
January, 1970
NGL 22-009-003

Submitted by:
Nicholas J. Grant, Supervisor
Harish Dalal
Manohar Grewal
Christina Jansen
Donald Kenton
Michael Lebo
William Schilling

To
National Aeronautics and Space Administration
Washington, D. C. 20546

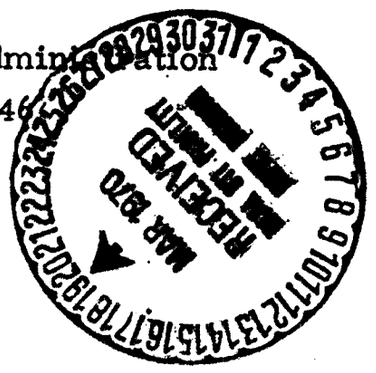

TABLE OF CONTENTS

LIST OF TABLES

LIST OF FIGURES

INTRODUCTION

The two-pronged approach of this program on Mechanisms of Alloy Strengthening remains entirely valid, and has in the past year found much additional support.

In the one approach, namely, via the utilization of ultra-fine refractory, stable dispersions, a number of conclusions can now be made, all of which are supportable by clear, reproducible, experimental data. For example:

1) There are processing techniques for the production of OD alloys which should be inexpensive, permit the preparation of a wide range of alloy compositions, and are attractive for commercialization. This was demonstrated in the recently reported work of Schilling and Grant with surface plus internally oxidized, fine flake powders. The initial studies were done with Cu-Al-Al_2O_3 alloys, and are now being repeated with complex Ni-base alloys, described in this report. Other simple alloy processing methods should be studied because this is where the real progress and economic justification will become evident.

2) In heat resistant alloys containing chromium as the basis for oxidation resistance; the presence of Cr_2O_3 is decidedly detrimental to alloy strength and stability much above 1500 degrees F. This is now evident from the results reported by Dalal, and confirmed by Grewal, both of our laboratory (see their reports below).

3) OD Ni alloys appear to respond more effectively to cold work after extrusion than either Fe or Cu base OD alloys. DuPont data would suggest that cobalt also responds effectively. Accordingly, effects of texture strengthening should be examined in the OD Ni alloys.

4) Combined solid solution strengthening plus cold work strengthening of OD alloys is clearly the correct approach for achieving an excellent combination of low temperature and high temperature strength, as evidenced by Al-Mg-Al_2O_3 alloys (Bufferd and Grant), Cu-Al-Al_2O_3 and Cu-Ni-Al-Al_2O_3 alloys reported by Schilling and Grant.

5) If still higher room temperature properties are desired (but at the expense of the very high temperature properties), a dispersoid other than an oxide is indicated. This is indicated from the work reported below by Kenton for Ni-base titanium carbide dispersion strengthened alloys. Note that the 1800 degrees F properties are attractive (in view of the high tension strength at room temperature), but not up to that for TD-Ni, for the time being.

6) Important property improvements were shown right from the start with splat produced aluminum alloy 2024-T4. We expect further improvements as a result of further structure refinements, as reported below. In view of the excellent hot working behavior of the splat powder compact, and the excellent ductility in the T4 condition, a more highly alloyed system is indicated for the

next effort. The use of rapidly quenched alloy powders looks like a sure winner for high strength alloy systems.

More regarding these observations will be found in the individual project accounts in the balance of the report.

I. STRENGTHENING THROUGH FINE PARTICLE DISPERSION

1. The Role of Cr_2O_3 Contamination on the Stability of Stainless OD Alloys

This project was originated with the aim of developing an oxide dispersed (OD) alloy which would possess good oxidation resistance and retain its strength in the temperature range of 1800 to 2400 degrees F.

Two methods of producing such an alloy were investigated. In the first method, alloys of Ni-ThO_2, Ni-Mo-Co-ThO_2, Fe-BeO, and Fe-ThO_2 were made and chromized by the ONERA halide decomposition process. The alloys so produced are designated as the A-series alloys in Table I. Table I also includes Fe-BeO alloys (HG and HC) made in this laboratory to enable comparison with the chromized Fe-BeO alloy.

The B-series alloys were produced by mechanical blending of fine powders of austenitic type 316 stainless steel (SS) with ThO_2. The fine SS powder was made by attriting the as-received powder (av. size: 10 microns) in isopropyl alcohol. Blending of the ThO_2 with SS powder during attrition produced a dispersion of very fine quality. Dry blending gave a very poor dispersion due to the hygroscopic nature of ThO_2.

Due to the large surface of the fine stainless steel powder, significant amounts of Cr_2O_3 were formed as a surface oxide. Removal of Cr_2O_3 is quite difficult because of its thermodynamic stability. H_2 was used to reduce Cr_2O_3 at 2200 degrees F. It was found after extensive investigations that the rate controlling step in the reduction of Cr_2O_3 is the removal of H_2O and that accumulation of H_2O in the reduction chamber slows down the rate significantly. In order to overcome this problem, porous wafers having a thickness of 1/16 inch were made and subjected to H_2 reduction for 10 hours at 2200 degrees F. The end of the reaction was determined by use of an O_2-concentration galvanic cell using a Ni-NiO mixture as the reference electrode. ZrO_2 was used as the solid electrolyte for O_2 ions. The cell reactions were described in the July 1969 semi-annual report in considerable detail and will not be repeated here.

Table I

ALLOY DESIGNATIONS WITH CHEMISTRIES AND EXTRUSION CONDITIONS

Alloy Designation	Alloy Composition	Extr. Temp. (°F)	Extr. Ratio Red. of Area	w/o Cr_2O_3* in alloy
A(1)	Ni-20Cr-3.0v/o ThO_2	2000	22	1.00
A(2)	Fe-20Cr-3.0v/o ThO_2	2000	22	1.20
A(3)	Ni-20Cr-2.0v/o ThO_2	1800	22	0.80
A(4)	Ni-20Cr-30Co-5Mo-2.0v/o ThO_2	1800	22	1.30
A(5)	Fe-20Cr-3.0v/o BeO	1800	22	nil
A(6)	Ni-20Cr-2.0v/o ThO_2	2000	25	0.33
HB+	Fe-3.0v/o BeO	1560	17	nil
HC+	Fe-3.0v/o BeO	1800	17	nil
B(1)	ss**-5.0v/o ThO_2	2000	16	1.20
B(2)	ss -5.0v/o ThO_2	2000	16	1.03
B(3)	ss -5.0v/o ThO_2	1800	22	3.50
B(4)	ss -5.0v/o ThO_2	1800	22	1.96
B(5)	ss-21.5v/o Cr_2O_3	2000	25	15.00
B(6)	ss-17.5v/o Cr_2O_3	2000	25	12.00
B(7)	ss -5.0v/o ThO_2	2000	20	0.2

*methods for separating Cr_2O_3 and ThO_2 from thoriated stainless steel are given in Appendix I.

**ss - type 316 stainless steel

+alloys B and C made by Hunkeler

The use of an end point indicator avoids unduly long exposure of the alloy at the elevated temperatures required for complete Cr_2O_3 reduction. This minimizes the growth of the ThO_2 dispersion. The above mentioned wafer technique was used for alloy B(7). The average particle size of the stainless steel powder used for alloy B(7) was 1-2 microns. At the end of the reduction process it was found that the quantity of Cr_2O_3 in the alloy decreased from 20.6 w/o to 0.2 w/o whereas the average diameter of ThO_2 particles increased from 100 Å to 300 Å.

The details of the processing of the stainless steel powders for the B-series alloys are given in Table II along with the average size of the stainless steel powder used for each of the alloys. Once the powders were processed they were compacted into steel cans. The steel cans were evacuated, sealed and extruded under conditions given in Table I. The alloys in the A-series were received in the as-H_2-sintered cylindrical compacts. They were vacuum sealed in steel cans and extruded as shown in Table I.

The extruded alloys were evaluated using the following tests:

a) Annealing study: samples were cut from the extruded rods and annealed for one hour at 1800, 2000, 2200, 2375, and 2450 degrees F. Hardness was measured in Rockwell G units. Plots of hardness versus temperature are shown in Figure 1. X-ray back reflection Laue patterns were taken on the annealed samples to determine the recrystallization behavior.

b) Room temperature tensile testing was done on an Instron machine using a cross-head speed of 0.02 inch per minute. The results of the tests are tabulated in Table III.

c) Stress-rupture tests were conducted on well-aligned creep frames with a lever arm arrangement for load application. Extension was measured by a dial gage with a sensitivity of 10^{-2} inch. The temperature fluctuation in the furnaces used was measured to be $\pm$ 3 degrees F. The tests were carried out at 1500, 1800, and 2000 degrees F depending on the stability of the alloy. Alloy A(5) was tested at 1400 degrees F to enable comparison with alloys HB and HC. The results of stress-rupture tests are plotted in Figures 2 - 5 and tabulated in Table IV.

It is seen from the test results on the A-series alloys that these alloys have excellent room-temperature strength but poor elevated temperature stress-rupture properties (Figure 2). Metallographic examination revealed the presence of chromium rich islands in alloys A(1) to A(4). Surrounding the chromium rich islands were heavy concentrations of Cr_2O_3. Alloy A(6) did not possess the Cr inhomogeneity but the dispersoid size was found to be much too large (approx. 0.5 - 1.0 micron) to provide elevated temperature stability to the alloy. The

Table II

PROCESSING OF THE ALLOYS IN THE B-SERIES

Alloy	Attriting	Av. metal powder particle size (μ)	Blending ThO_2	H_2-reduction	Compacting into a mild steel extrusion billet on a 30 ton press
B(1)		10	with dry ss powder, in a Waring blender in batches of 200 g.	in a Vycor tube, using prepurified H_2, for 8 hrs. at 1400°F	load 30-tons, in batches of approx. 100 g.
B(2)		10	same as B(1)	done in a mild steel tube using prepurified H_2 for 12 hours at 2200°F	no compacting required, tube containing the sintered pellet was put directly into the extrusion billet
B(3)	4 days without recirculating the slurry	4-5	performed during attriting	same as B(1)	same as B(1)
B(4)	same as B(3)	4-5	same as B(3)	same as B(2), except that the sintering time was 24 hrs.	same as B(2)
B(5)	7 days with recirculation of the slurry	1-2	ThO_2 not added	same as B(1)	same as B(1)
B(6)	same as B(5)	1-2	ThO_2 not added	same as B(4)	same as B(2)
B(7)	same as B(5)	1-2	ThO_2 added as a colloidal suspension in distilled water during attriting	carried out on compacts 1/16 x 1 1/4 in. dia., using ultrahigh purity H_2, for 10 hrs. at 2200°F	H_2 sintered compacts broken into small pieces and compacted as in B(1)

Table III

ROOM-TEMPERATURE TENSILE TEST DATA

(one test per alloy)

Alloy	0.2% offset Y.S. (psi)	U.T.S. (psi)	% Elongation
A(1)	113,750	126,250	7
A(2)	53,750	75,000	9
A(3)	107,500	113,750	10
A(4)	162,500	167,500	5
A(5)	72,500	104,000	17
A(6)	112,000	131,000	13
HB	61,000*	73,700	18
HC	58,500*	73,700	20
B(1)	92,000	123,500	17
B(2)	43,600	82,400	22
B(3)	122,200	125,000	5
B(4)	62,500	88,000	16
B(5)	110,000	122,500	2
B(6)	57,500	70,700	7
B(7)	70,700	108,600	11
S+	50,000	80,000	50

S+ : wrought type 316 ss.

*lower yield strength. Values for upper yield are: HB - 81,000 psi

HC - 68,300 psi

Table IV

STRESS-RUPTURE DATA

Alloy	Temp. (°F)	Stress (psi)	Rupture life (hrs.)	% elongation	% reduction in area
A(1)	1800	5000	0.033	2.0	2.5
A(1)	1800	2000	>270	3.1	1.3
A(1)	1800	4000	0.82	1.8	0.6
A(1)	2000	3500	0.27	3.7	3.8
A(1)	2000	5000	0.0005	5.4	6.3
A(2)	1800	1500	0.06	6.6	1.3
A(2)	1500	1500	0.42	4.3	0.6
A(2)	1500	1000	6.6	1.8	1.6
A(2)	1500	2000	0.07	5.1	0.4
A(2)	1500	1250	1.7	2.3	1.3
A(3)	1800	5000	0.002	7.4	1.1
A(4)	1800	3500	0.01	10.8	16.9
A(5)	1400	8000	1.13	3.9	3.1
A(5)	1400	7000	1.98	2.6	3.1
A(6)	1500	2000	12.3	6.5	21
A(6)	1500	5000	0.033	12.2	15
A(6)	1500	3000	0.96	8.1	17
B(1)	1800	5000	0.22	7.1	0.6
B(1)	1800	2200	1.77	10.4	1.9
B(1)	1800	1500	4.4	12.8	3.1
B(1)S*	1800	1500	4.9	9.7	1.6

* S = 30% reduction in area by room temperature swaging.

Table IV (cont'd.)

Alloy	Temp. (°F)	Stress (psi)	Rupture life (hrs.)	% elongation	% reduction in area
B(2)	1800	2500	3.9	5.9	3.1
B(2)	1800	4000	0.71	4.9	3.8
B(2)S	1800	4000	0.24	2.5	0.62
B(2)S	1800	2500	2.7	6.3	3.1
B(2)	1500	10,000	2.0	5.1	5.6
B(2)	1500	5000	5.9	3.4	3.1
B(2)S	1500	10,000	2.2	5.4	5.0
B(2)S	1500	5000	7.9	7.7	5.0
B(3)	1800	5000	0.033	- *	-
B(3)	1800	3500	0.08	-	-
B(3)	1800	2500	0.25	5.8	5.0
B(3)	1500	5000	10.6	5.2	5.0
B(3)	1500	10,000	1.4	-	4.0
B(4)	1500	5000	6.4	16.9	2.5
B(4)	1500	8000	1.5	8.7	5.0
B(4)	1500	2500	56	19.2	2.3
B(4)	1800	5000	0.08	7.4	1.1
B(4)	1800	2500	0.92	3.1	1.9
B(4)	1800	1500	5.6	2.7	2.1
B(6)	1500	15,000	1.05	8.2	1.9
B(6)	1500	10,000	4.0	7.1	2.8

*Some of the values for elongation could not be obtained due to the condition of the specimens after the test.

Table IV (cont'd.)

Alloy	Temp. (°F)	Stress (psi)	Rupture life (hrs.)	% elongation	% reduction in area
B(6)	1500	5000	38.0	-	5.0
B(5)	1500	5000	1.5	7.9	5.0
B(5)	1500	3000	12.8	-	4.0
B(5)	1500	4000	5.0	9.3	4.8
B(7)	1800	5000	121.0	3.8	3.9
B(7)	1800	8000	1.05	15.0	8.4
B(7)	1800	6500	7.6	12.3	7.4
B(7)	2000	5000	1.0	16.6	9.3
B(7)	2000	4000	9.2	13.7	8.8
B(7)	2000	3000	145.0	7.1	6.9

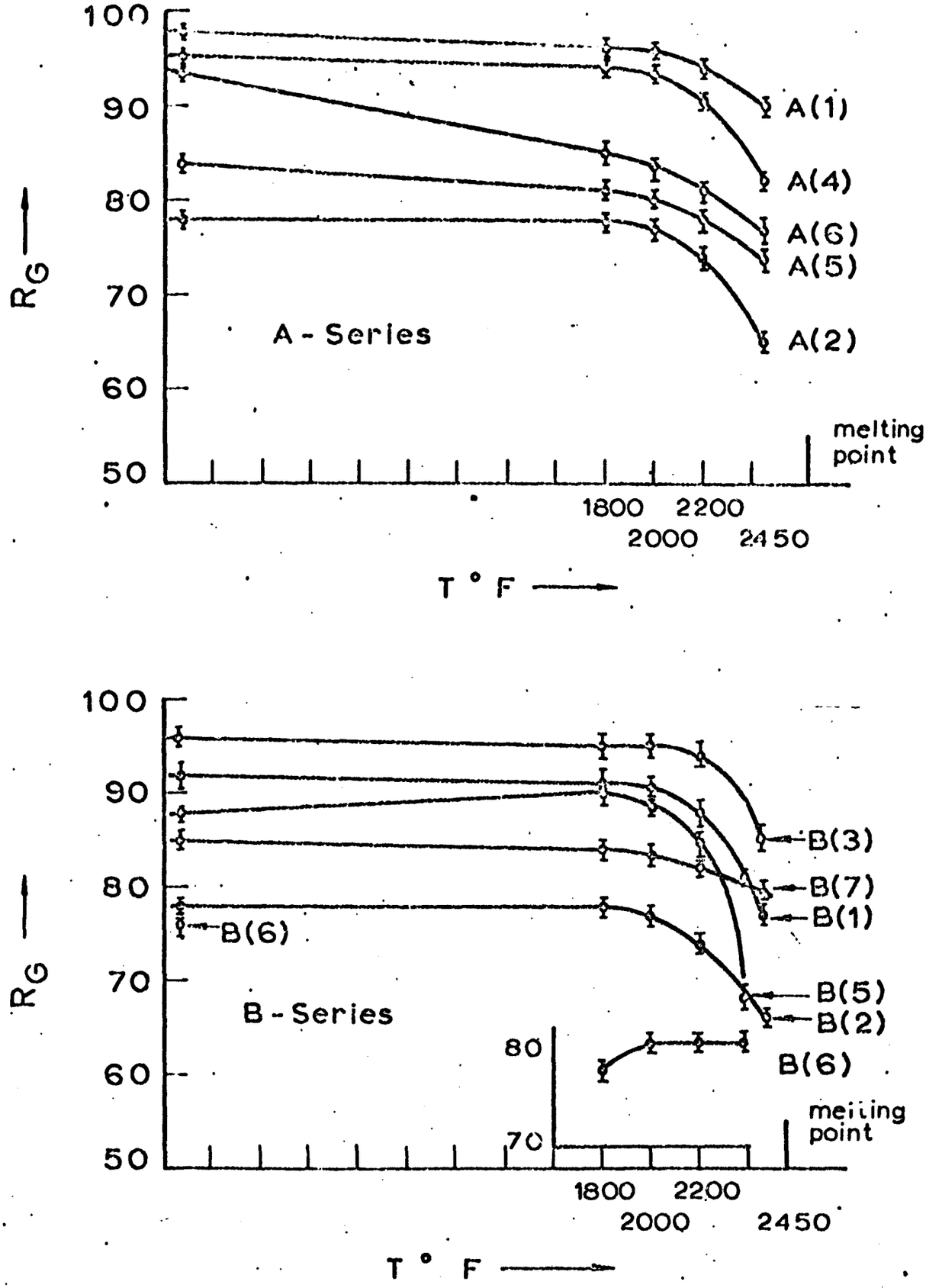

Figure 1. Hardness versus temperature at room temperature (1 hour holding time) for OD stainless steel alloys.

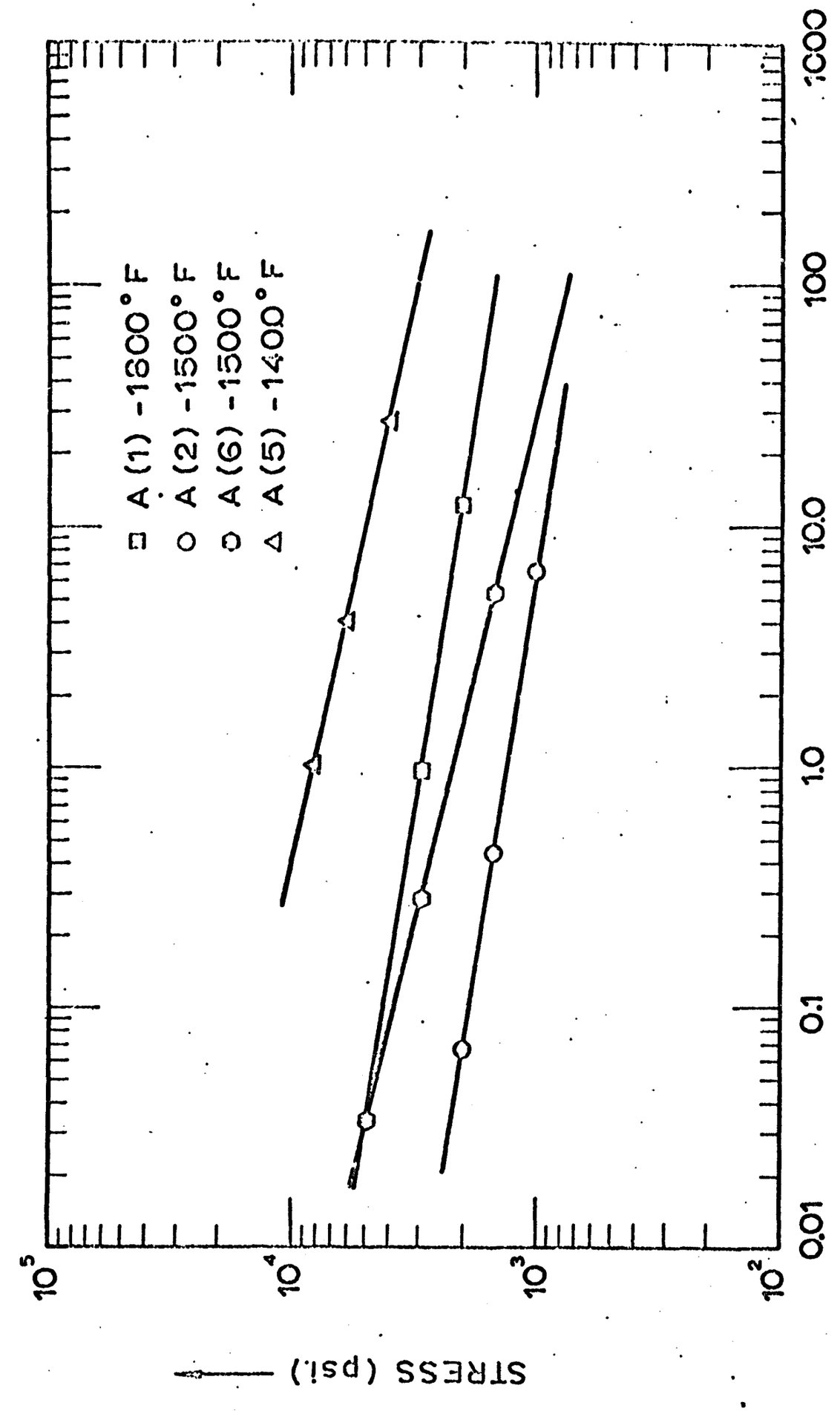

Figure 2. Log stress versus log rupture time for A-series alloys from 1400-1800 degrees F.

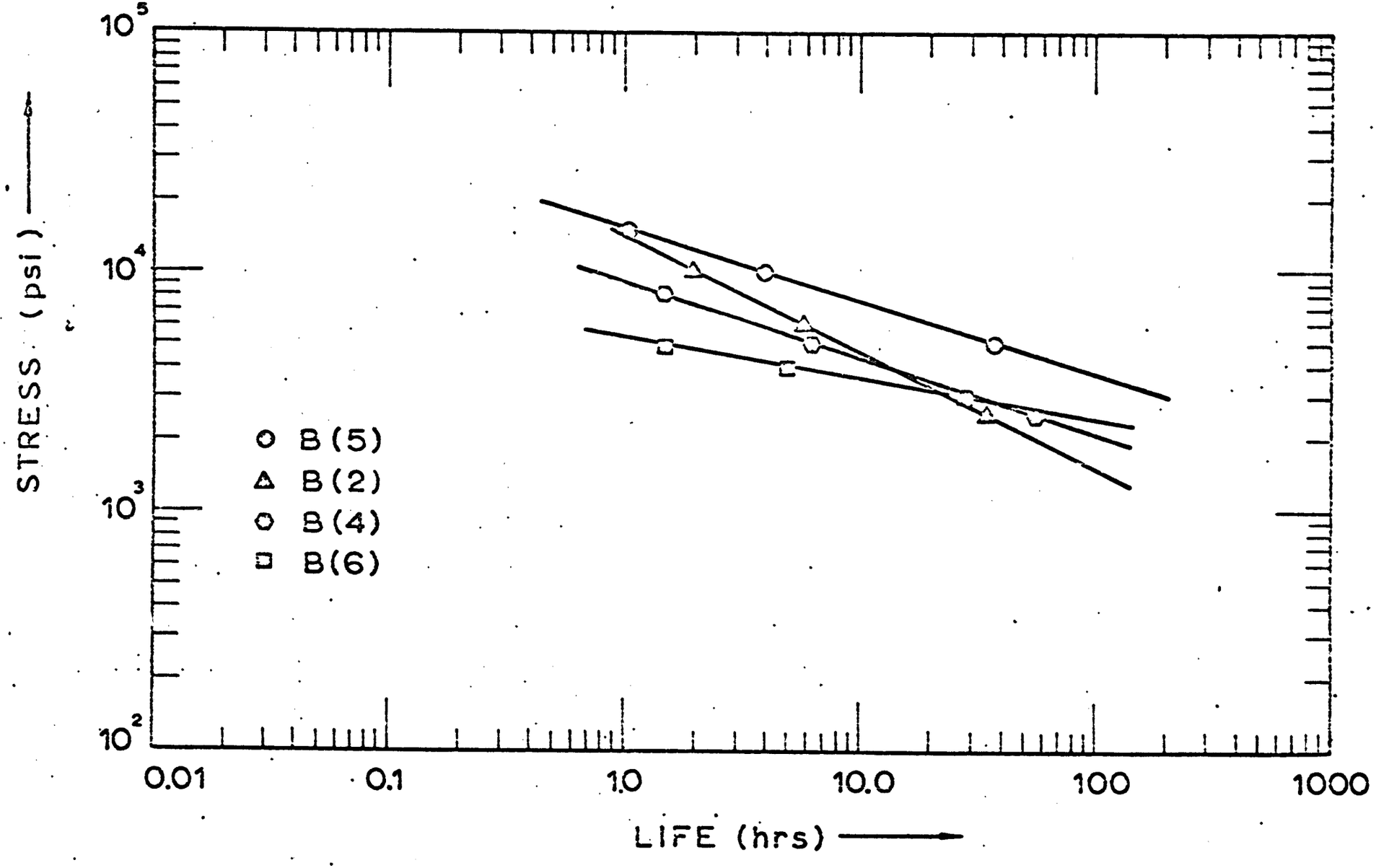

Figure 3. Log stress versus log rupture time for B-series alloys at 1500 degrees F.

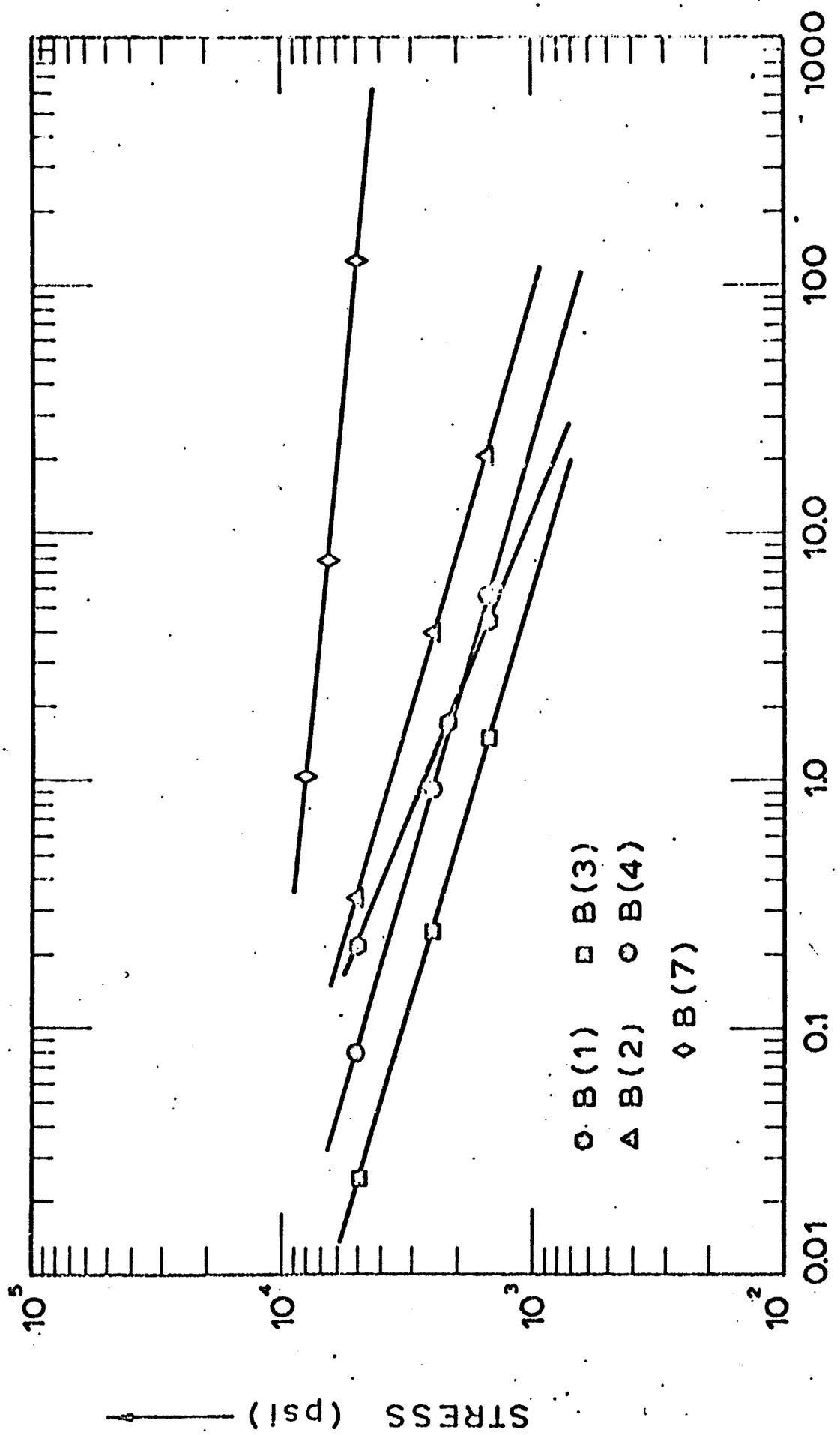

Figure 4. Log stress versus log rupture time for B-series alloys at 1800 degrees F.

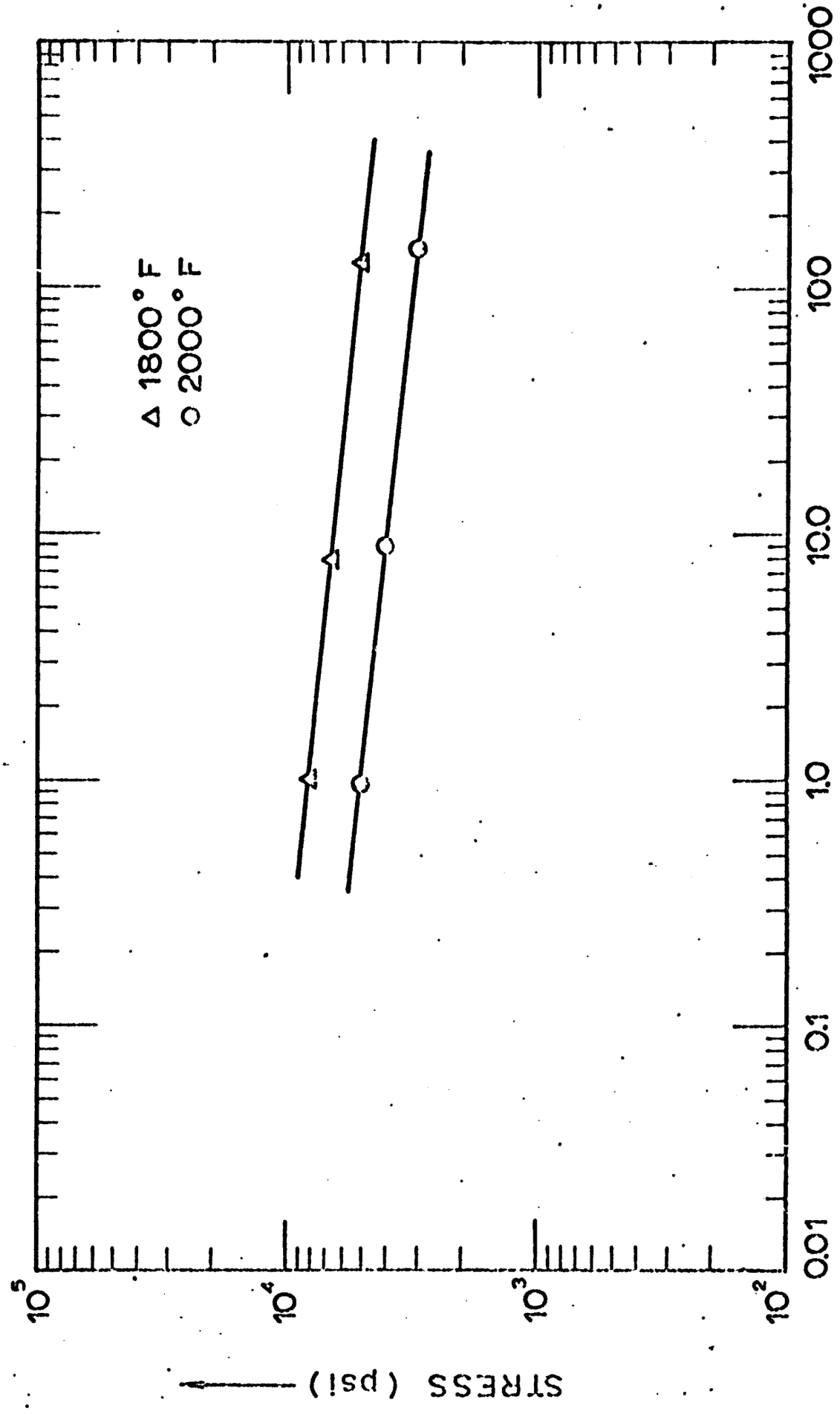

Figure 5. Log stress versus log rupture time for B(7) at 1800 and 2000 degrees F.

recrystallization temperature for all the A-series alloys was found to be 2000 degrees F. The halide decomposition process for adding chromium to OD alloys remains an attractive process since it offers an effective means of avoiding Cr_2O_3 contamination of the alloy.

The B-series alloys also have excellent room-temperature strength but poor elevated temperature stress-rupture properties except for B(7). Alloys B(5) and B(6) were made without any ThO_2 additions to determine the effect of Cr_2O_3 alone on the alloys. Since alloy B(6) underwent H_2 sintering for 24 hours at 2200 degrees F, it was lower in Cr_2O_3 (Table I) than B(5). On the other hand, the size of Cr_2O_3 is about 2 microns in B(5) and about 6 microns in B(6). Metallographic examination of a sample of B(5) annealed at 2375 degrees F showed that the Cr_2O_3 particles have begun to disintegrate and dissolve in the matrix. A sharp drop in hardness of B(5) can be observed at this point in Figure 1. Though the volume fraction of Cr_2O_3 in B(6) is slightly decreased after a one hour anneal at 2375 degrees F, there are no signs of disintegration of Cr_2O_3, and the sharp drop in hardness is not observed. This indicates that the presence of Cr_2O_3 would be detrimental to the elevated temperature properties of the alloy as it can dissolve into the matrix and reprecipitate on already existing ThO_2 particles. This increases the actual size of the dispersoid causing a degradation of the stress-rupture properties of the alloy. The finer the size of the Cr_2O_3 the worse would be its effect on the stress-rupture properties. Further comparison of alloy B(1) with B(2) and B(3) with B(4) shows that alloys B(2) and B(4), which are lower in Cr_2O_3, have better stress-rupture properties. However, alloys B(1), B(3), and B(5) have better room-temperature tensile strength because of their higher total oxide (Cr_2O_3 + ThO_2) content.

The fracture surfaces of some of the tensile specimens were studied in a scanning electron microscope. The dimpled nature of the surface indicated a ductile mode of fracture of these alloys.

The influence of Cr in solution on ThO_2 was investigated by annealing samples of TD-Ni and TD-NiCr at 2372 and 2462 degrees F for 100, 200, and 300 hours. Extraction replicas of the annealed samples were made and photographed at 40,000X in a Hitachi HU-11 electron microscope. The average size of ThO_2 ($\bar{a}$) was computed for each of the annealed samples using a Quantimet. The results are tabulated in Table V and plotted in Figure 6. These results were used to compute the activation energy (Q_c) and the rate constant (k) for the coarsening of ThO_2 using the theory of diffusion controlled coarsening of precipitates in a matrix by Lifshitz and Slyzov.

Table V

Alloy	Annealing time (hrs.)	Annealing temp. (°F)	Av. dia. $\bar{a}$ (mm)	Av. dia. $\bar{a}$ (Å)	$(\text{Av. dia.})^3$ $\bar{a}^3$ (mm^3)
TD-Ni	100	2372	1.74	435.0	5.25
	200	2372	1.79	447.5	5.75
	300	2372	1.84	480.0	6.25
	100	2462	1.83	457.5	6.15
	200	2462	1.96	490.0	7.55
	300	2462	2.09	522.5	9.15
TD-NiCr	100	2372	1.65	412.5	4.5
	200	2372	1.69	422.5	4.85
	300	2372	1.73	432.5	5.2
	100	2462	1.71	427.5	5.05
	200	2462	1.81	452.5	5.9
	300	2462	1.90	475.0	6.9

TD-Ni: $\bar{a}_o$ = 1.68 mm at 40,000x = 420 Å

TD-NiCr: $\bar{a}_o$ = 1.60 mm at 40,000x = 400 Å

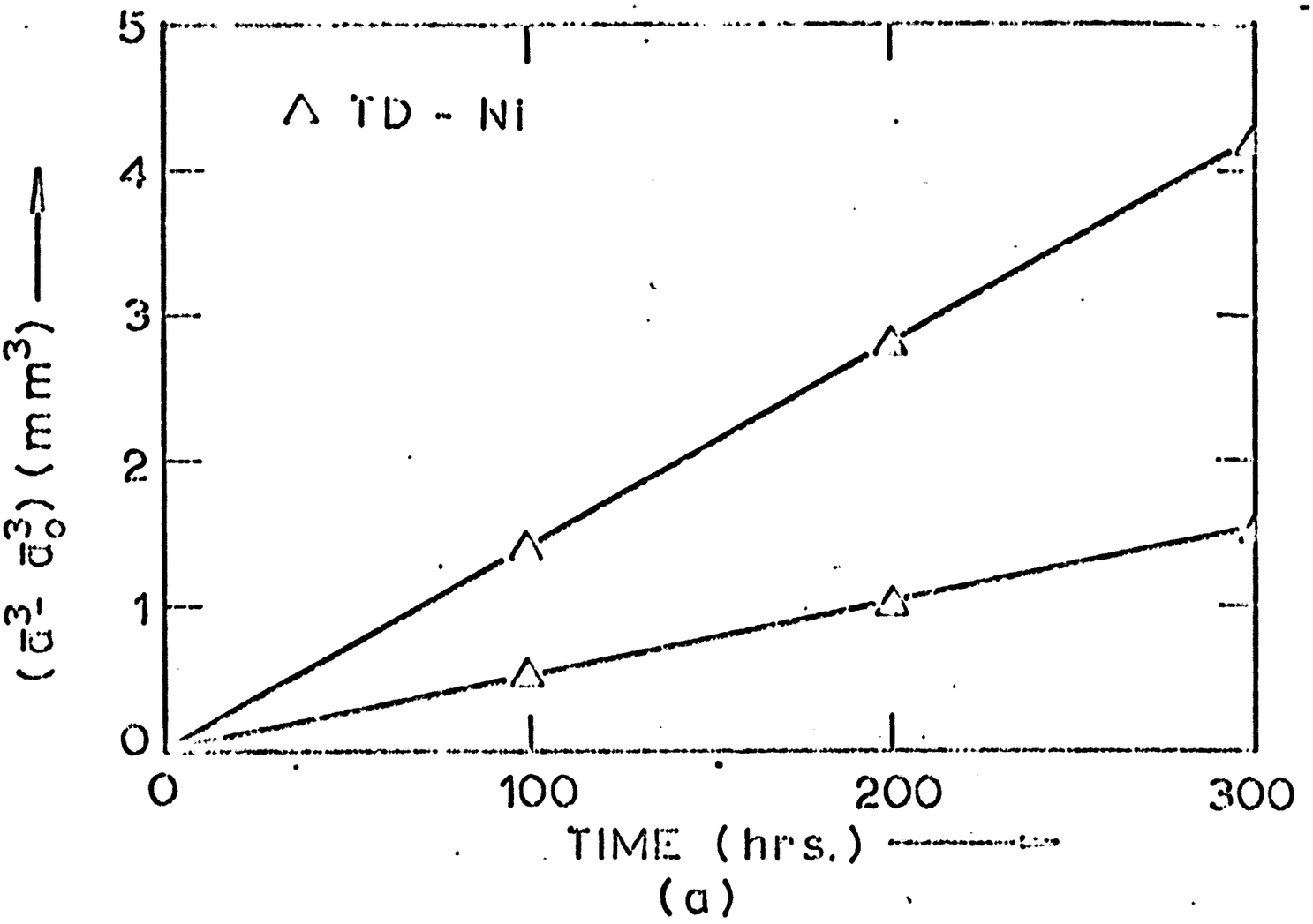

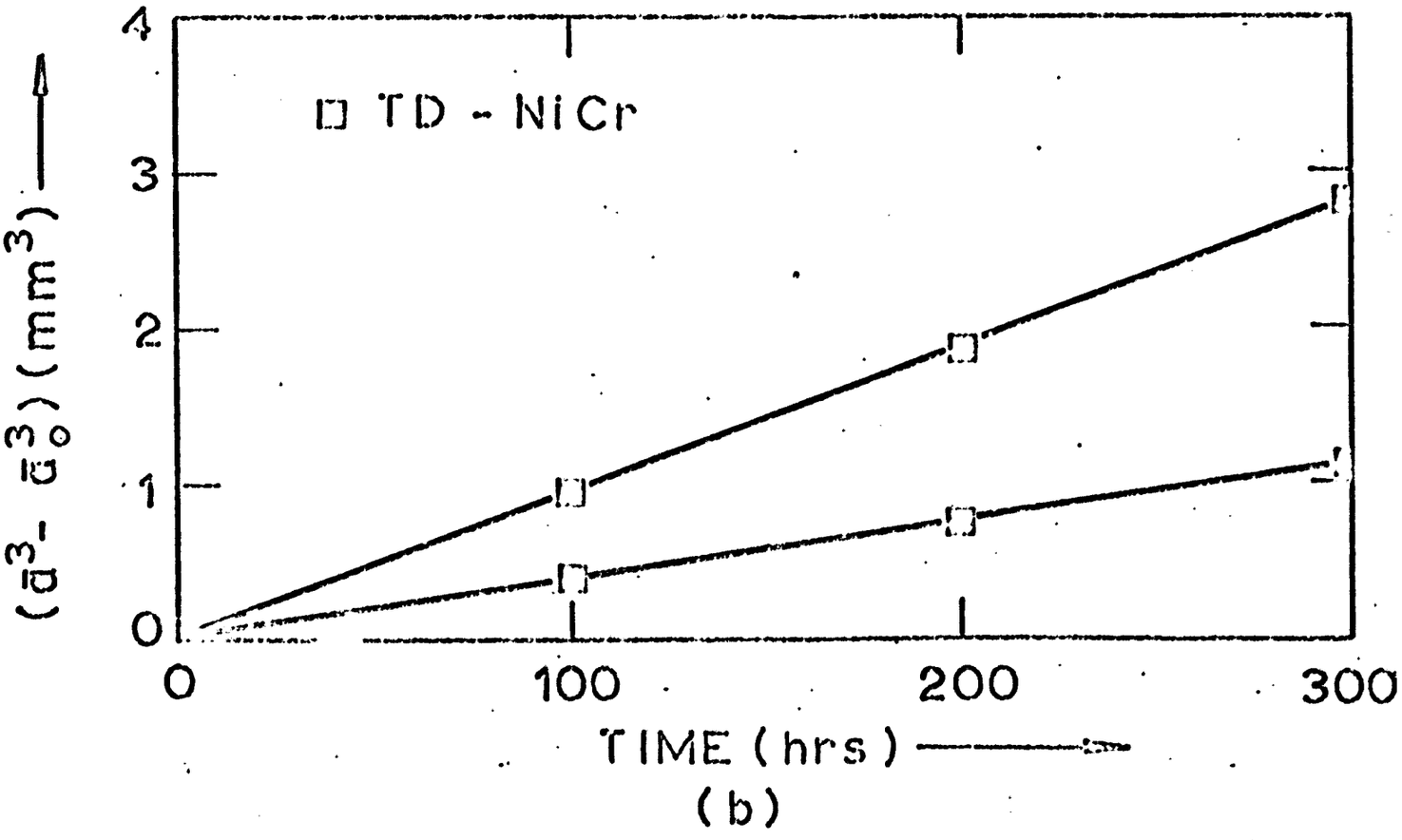

Figure 6. Coarsening of ThO_2 for TD-Ni and TD-NiCr.

According to the theory

$$\bar{a}^{-3} \cdot \bar{a}_o^{-3} = kt \quad (1)$$

$$k = k_o \exp \left[- Q_c/RT \right] \quad (2)$$

$$Q_c = Q_d + Q_s + RT \ln T \quad (3)$$

where

$\bar{a}$ = av. dia. of the precipitates after time t at temperature T

$\bar{a}_o$ = initial av. dia. of the precipitates

Q_c = activation energy for coarsening of the precipitate

Q_d = activation energy for diffusion of the slowest moving component of the precipitate

Q_s = activation energy for solution of the slowest moving component of the precipitate

k = rate constant

k_o = constant and R = gas constant

The value of k was computed from Figure 6 using equation (1) and that of Q_c from Figure 7 using equation (2). The values are given below:

Alloy	Activation Energy	Rate Constant $k(cm^3/sec) \times 10^{22}$ at	
	Q_c (k cals.)	2372 F	2462 F
TD-Ni	105	0.52	1.51
TD-NiCr	96	0.38	0.96

It is seen that the presence of Cr lowers the activation energy for coarsening of ThO_2, but the overall rate of growth decreases. The presence of Cr is therefore not detrimental to the alloy.

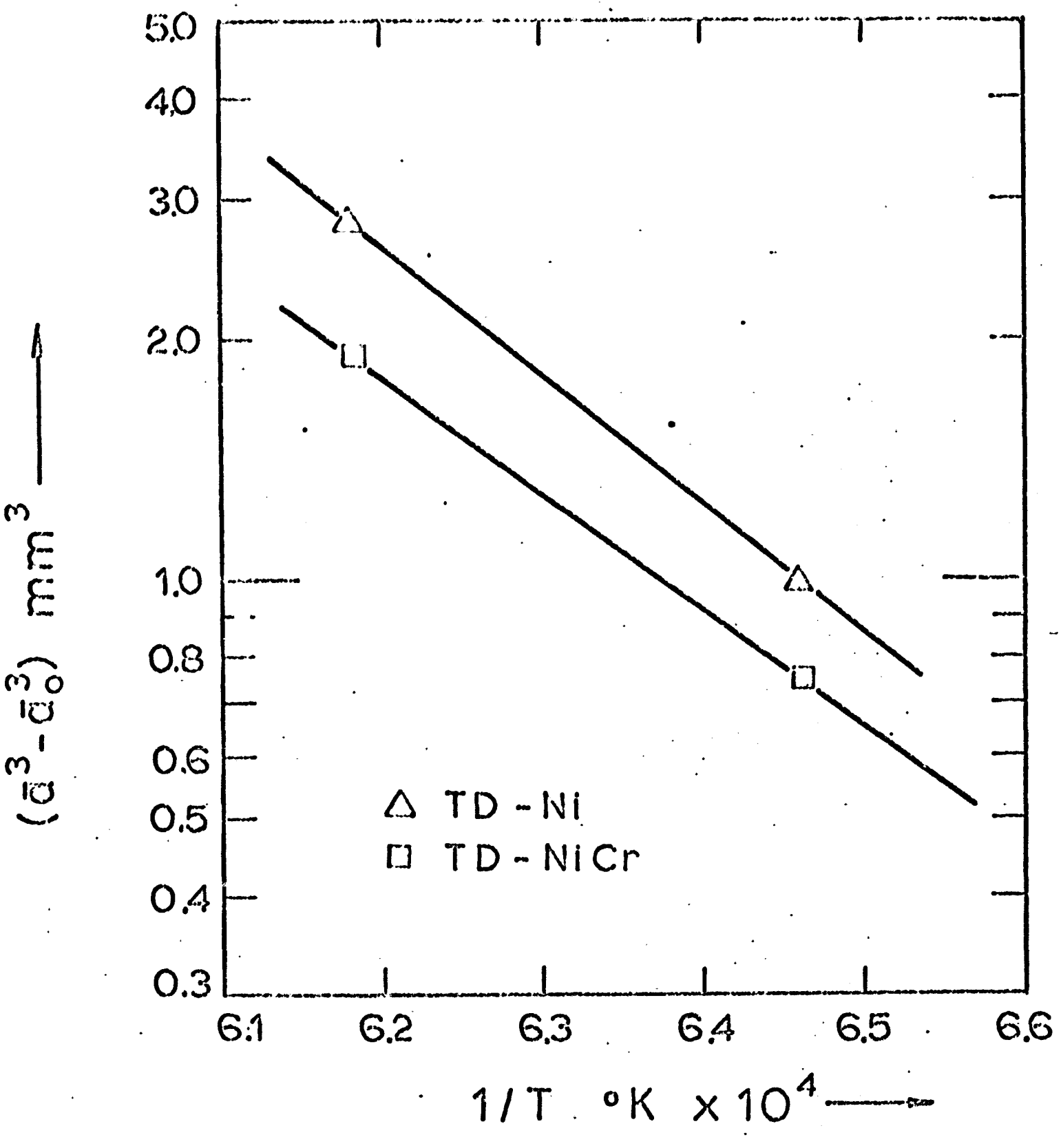

Figure 7. Coarsening of TD-Ni and TD-NiCr versus reciprocal temperature.

2. Ni-BeO Alloys Produced by Internal Oxidation

Mechanical Properties of the Ni - 1 v/o BeO Alloy - In the previous report room temperature tensile data and hardness versus annealing temperature (one hour holding time) data for a Ni - 1 v/o BeO alloy, in the as-extruded condition, were reported. This alloy was subjected to 30, 60, and 70 percent reduction of area by cold swaging with one hour intermediate anneals at 1500 degrees F after each 10 percent reduction. Effects of these thermomechanical treatments on room temperature tensile properties are given in Table VI.

Table VI

Effects of Thermomechanical Treatment on Tensile Properties of a Ni - 1 v/o BeO Alloy at 70 degrees F

Condition	U.T.S. (psi)	Y. S, 0.2% (psi)	Elongation, %
As extruded	82,500	70,000	20.0
30% cold worked	90,460	89,100	15.0
60% cold worked	91,080	89,172	10.5
70% cold worked	91,200	90,000	9.0

Not unexpectedly, the U.T.S. and Y.S. increase with increasing cold work and ductility decreases; the effects after about 30 percent reduction are quite small. The Y.S. approaches the U.T.S. after about 30 percent reduction.

The effect of annealing temperature (one hour holding time at temperature) on the room temperature hardness with increasing cold work is shown in Table VII.

Table VII

Room Temperature Hardness Versus Annealing Temperature for the Ni - 1 v/o BeO Alloy

Rockwell B	Degrees F				
Condition	70	1832	2057	2192	2462
As extruded	95.5	94.5	92.5	88	73
30% cold work	99.0	96.0	87.5	80	-
60% cold work	98.0	94.5	87.5	80	-
70% cold work	97.0	93.5	87.0	81	-

As seen from Table VII, additional cold work after extrusion appears to affect adversely alloy stability, determined by hardness versus annealing temperature studies at 2057 degrees F and higher, with little difference emerging after 30 or 70 percent cold work; however, there was a marked improvement on stability with increasing cold work as indicated by the very flat slopes of log stress versus log rupture type plots (see Figures 8, 9, 10), and by the increase in activation energy for creep (see Table IX). The stress rupture data are given in Table VIII.

The stress for 100-hour rupture life at 1500 degrees F increased from 4600 psi for the as-extruded material to 11,500 psi after 60 percent cold work, and at 1800 degrees F from only 920 psi to 5,600 psi. These results confirm the large benefits which nickel-base oxide dispersed alloys derive in terms of high temperature rupture strength from additional extensive cold work.

Table VIII

Creep Rupture Data for a Ni - 1 v/o BeO Alloy

Condition	Test Temperature, degrees F	Stress for 100-Hour Rupture Life, psi
As extruded	1500	4,600
30% cold work	1500	7,450
60% cold work	1500	11,500
As extruded	1800	920
60% cold work	1800	5,000
70% cold work	1800	5,600
60% cold work	2000	2,400
70% cold work	2000	3,500

Wilcox and Clauer have investigated the steady state creep rate in TD-Ni and have shown that the steady state creep rate ($\dot{\varepsilon}$) can be emperically related to stress, as follows:

$$\dot{\varepsilon} = A\sigma^{n} \quad \mathrm{EXP}\left(-\frac{Q_c}{RT}\right) \tag{4}$$

where

σ = applied stress

Q_c = activation energy for creep

A and n are constants

R = gas constant

T = temperature in k degrees

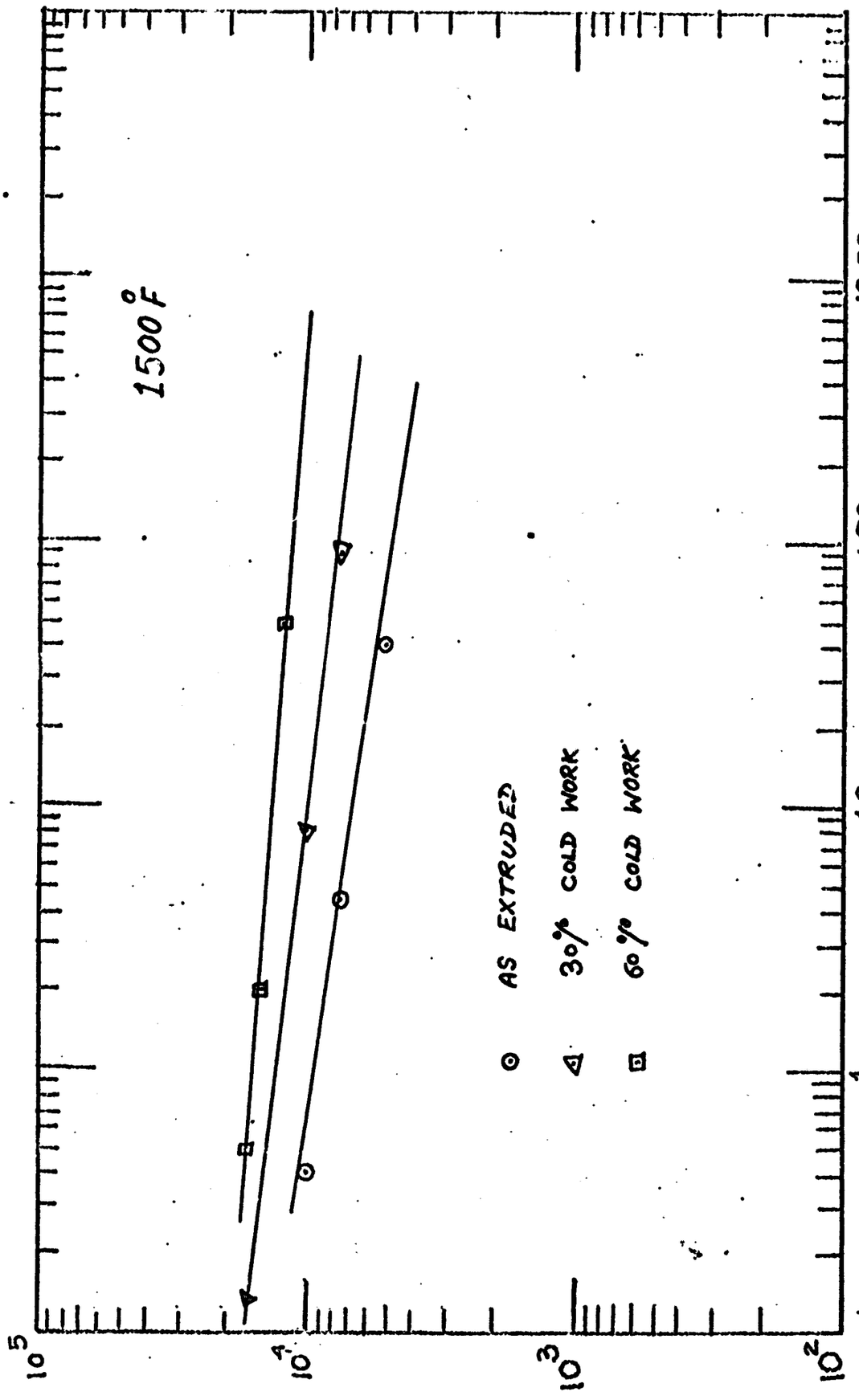

LOG STRESS VERSUS LOG RUPTURE TIME AT 1500°F FOR Ni-1 Vol% BeO ALLOY AS A FUNCTION OF COLD WORK.

Figure 8

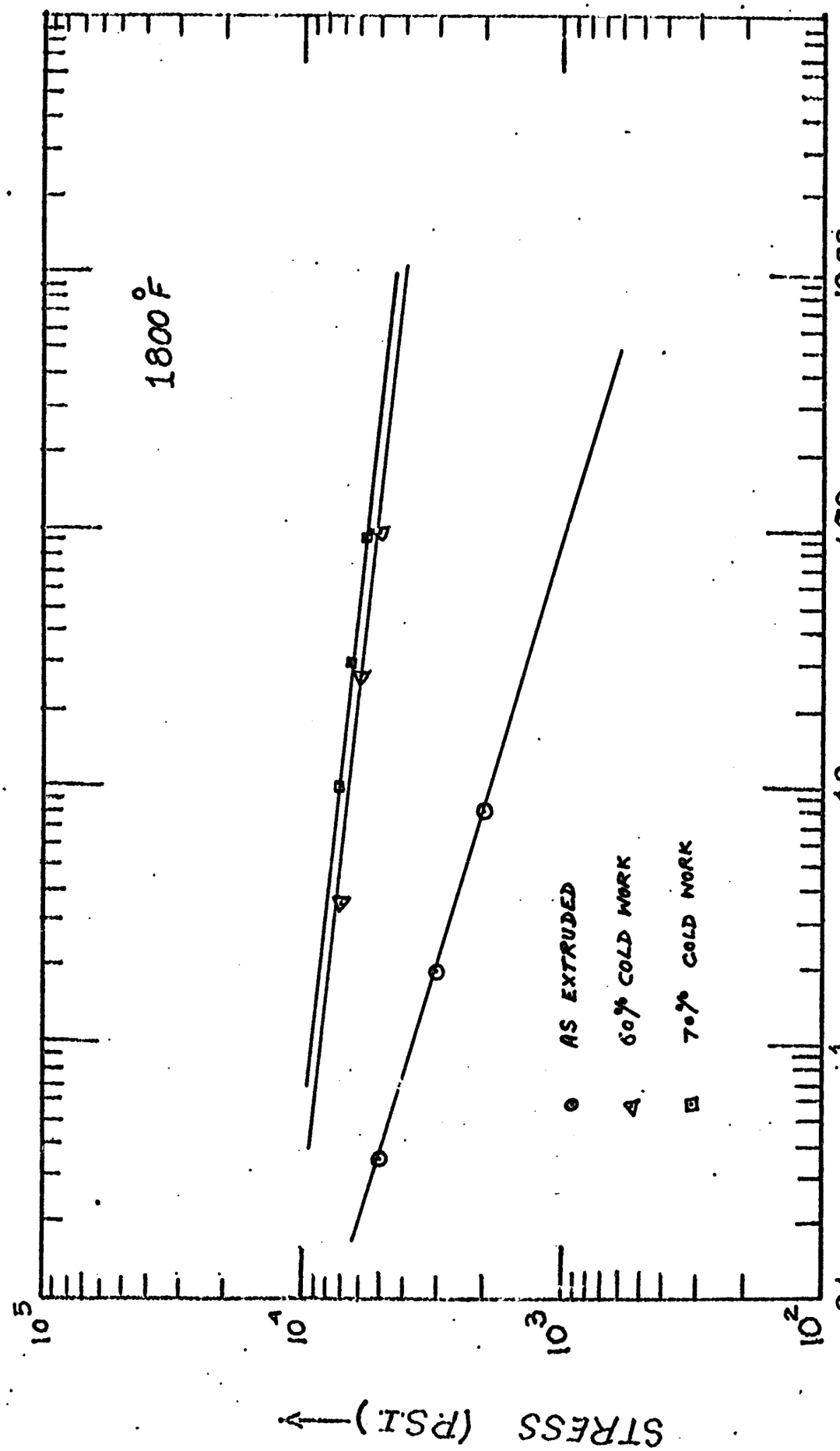

LOG STRESS VERSUS LOG RUPTURE TIME AT 1800°F FOR Ni-1 Vol% BeO AS A FUNCTION OF COLD WORK.

Figure 9

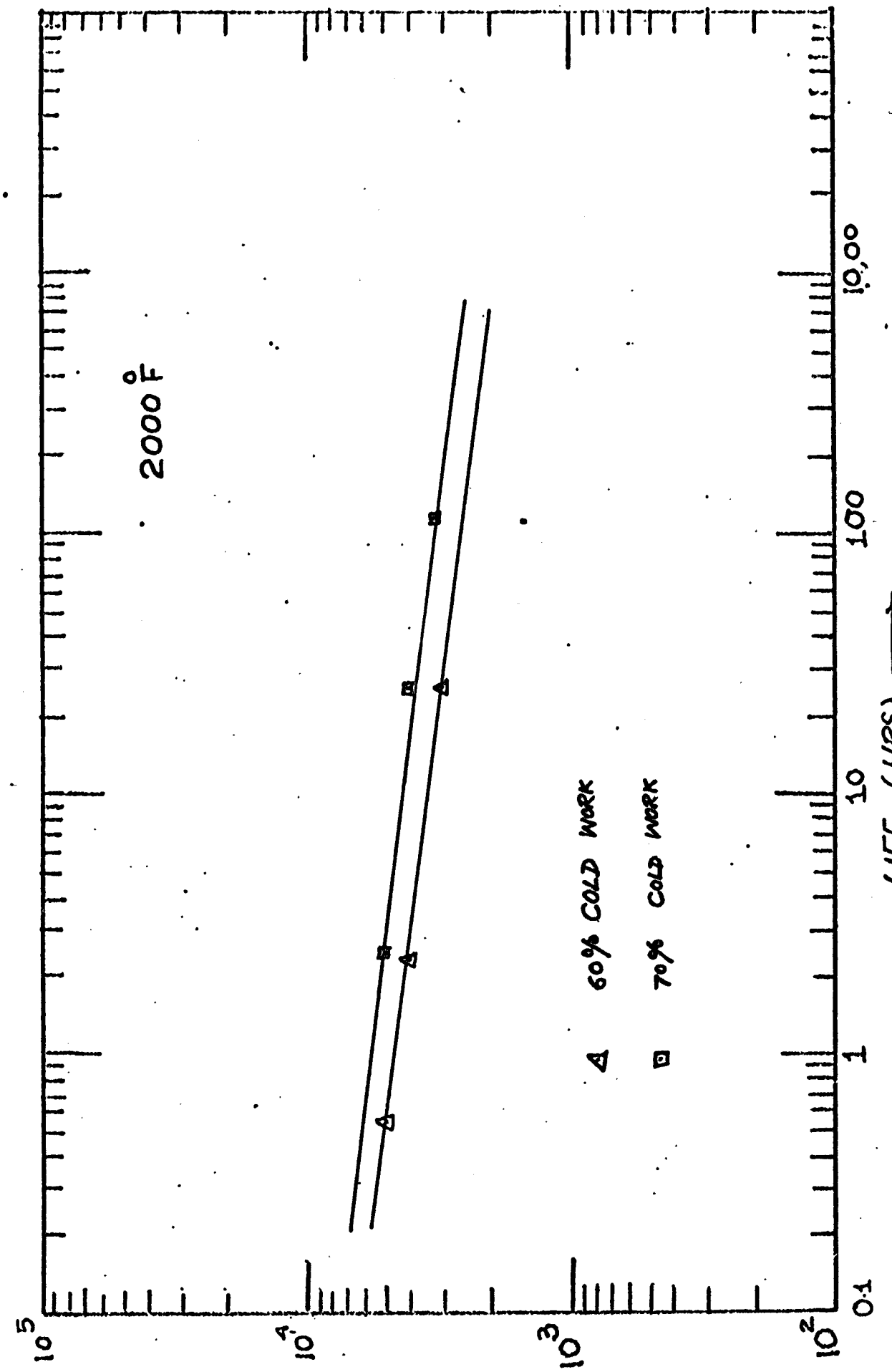

LOG STRESS VERSUS LOG RUPTURE TIME AT 20[illegible]°F FOR Ni-1Vel% Be0 ALLOY AS A FUNCTION OF COLD WORK

Figure 10

The stress dependence exponent (n) can be determined from $\ell n \sigma$ versus ℓn rupture time or $\ell n \dot{\varepsilon} + \frac{Q_c}{RT}$ versus $\ell n \sigma$ plots, and the activation energy (Q_c) can be obtained by determining the creep rates at two different temperatures (differential temperature method) using equation (5):

$$Q_c = \frac{R \ \ell n \ \dot{\varepsilon}_s^2 / \dot{\varepsilon}_s^1}{\frac{1}{T_1} - \frac{1}{T_2}} \qquad (5)$$

Such determinations were made for the Ni - 1 v/o BeO alloy after various amounts of cold work and are compared with the results of Wilcox and Clauer for TD-Ni, in Table IX.

Table IX

Values of Stress Exponent (n) and Activation Energy for Creep (Q_c)

Alloy	Condition	n	Q_c	K cal/mole
TD-Ni	(a) as received, 90%c.w.	40		190
Ni-2 v/o ThO_2	(b) recrystallized	119 for high σ 15 for low σ		235
Ni- 1 v/o BeO	(a) as-extruded (20:1 extrusion ratio at 1800 degrees F)	6.0 for low σ		99
	(b) plus 30% c.w.	8.0 for low σ		175
	(c) plus 60% c.w.	14.0 for low σ		250

The activation energy of the as-extruded alloy is slightly higher than that of self diffusion energy (65 k cal/mole) in pure Ni, and it increases with increasing cold work. The same trend is found for the stress exponent (n). The slope of log stress versus log rupture time (Figures 8, 9, 10) became flatter with increasing cold work, again indicating the importance of thermo-mechanical treatment as a means of increasing the high temperature creep resistance of OD alloys.

Transmission electron microscopy is being used to gain further information on the role played by stored energy. The Ni - 1v/o BeO alloy has been successfully thinned after several months of search; the thinning method works equally well for the highly cold worked alloys. As-extruded material shows a high dislocation density and an absence of a cell structure. A cell structure starts to form with 30 percent cold work and is developed with further cold work - annealing cycles. The dislocation density increases and the subcells become smaller

with increasing cold work. Many oxide particles are seen to be present at cell boundaries; often, dislocation-particle-networks and dislocation loops are observed. The particles seem to pin dislocations and subboundaries. The specimens which have been creep tested are being thinned now, and the results will be forthcoming soon.

Reduction of Cr_2O_3 - It was mentioned in the previous report that 0.8 to 0.9 w/o Cr was picked up as contamination during ball milling. Chemical analysis of attrited powder shows about 30 percent total oxygen, which indicates that most of the powder is in oxide form. Since Cr_2O_3 adversely affects the stability of these alloys, it would be desirable to eliminate it or reduce it to Cr.

NiO can be reduced readily in dry hydrogen in 24 hours at 1200 degrees F, 6 hours at 1380 degrees F, or 1 to 2 hours at 1560 degrees F. During reduction of NiO, chromium oxide combines with BeO to form the spinel $BeCr_2O_4$, confirmed by X-ray analysis. It might be mentioned that $BeCr_2O_4$ peaks are not found in as-attrited powder, they appear only after the reduction process, the amount of the spinel increasing with increasing reduction temperature. Since Cr_2O_3 and Cr have high vapor pressure, an attempt was made first to eliminate Cr_2O_3 by heating in high vacuum. Powder, prior reduced to eliminate nickel oxide, was compacted into a thin wafer and heated in vacuum of better than 1×10^{-6} mm Hg at 2200 degrees F for 1, 4, and 8 hours. The results are summarized in Table X. It is evident from Table X that Cr_2O_3 can not be eliminated by heating in high vacuum. X-ray analysis indicated, on the contrary, formation of more $BeCr_2O_4$ as its peaks become intense and the Cr_2O_3 peaks were reduced considerably in intensity.

Table X

Effect of High Vacuum Treatment on Cr_2O_3 Content

Reduction Run #	Temperature, degrees F	Time hours,	Total O_2 content w/o	Total Cr_2O_3 content w/o
Initially NiO reduced pellet	-	-	0.55	1.2
1	2200	1	0.54	1.12
2	2200	4	0.56	1.10
3	2200	8	0.55	1.20

Next, attrited powder was made into thin wafers, 1 1/4" dia. x 1/16" thick, weighing about 3 grams. Twenty five of these wafers were staked in a tungsten coated Al_2O_3 coil and put in a horizontal, high purity Al_2O_3 boat. The reduction was done in two steps: first at 1380 degrees F for 24 hours, and then for 6 hours at 2200 degrees F in a horizontal Harper furnace in H_2 with dew point less than -87 degrees F. A small furnace and reduction unit was built for low temperature reduction to increase the efficiency of the process and to save time since two furnaces could be run simultaneously. Vacuum tight end caps were designed for the high temperature reduction furnace; a vacuum of hetter than 10 microns could be reached in 10-15 minutes. The system was fully vacuum and gas tight.

Twelve preliminary reduction runs were made to optimize the reduction conditions. X-ray studies and a scanning electron microscope were used to follow changes in oxide particle size and sintering process, respectively. The results of these runs are summarized in Table XI. It was clear from these runs that the purity of H_2 gas was critical. All final reduction runs were made with H_2 of better than - 87 degrees F dew point and 1 ppm of oxygen. Complete reduction of the spinel was not achieved. Chemical analysis showed that 0.21 w/o Cr_2O_3 was left unreduced, which was combined with BeO or existed as $BeCr_2O_4$ spinel (X-ray studies). The amount of BeO in the spinel corresponding to the above Cr_2O_3 is only 0.013 w/o versus about 0.10 w/o Be in the form of BeO. Since the amount of spinel is quite small and appears to be quite stable, it should not have adverse effects on the creep rupture properties.

Alloy Preparation in Progress

a) Attrition - About 2 pounds of the Ni - 1 v/o BeO alloy powder was reduced in the form of thin wafers, as described above, in batches of 25 wafers (about 80 grams per charge) and is ready for extrusion.

Alloy #2 (Ni - 2 v/o BeO) is being reduced by this technique now.

Five pounds of -100 mesh powder of #3 alloy (0.30 w/o Be, 4.5 Mo, and balance Ni) has been attrited and is being reduced now.

Alloy #4 with the same Be and Mo contents as #3, plus 30 w/o Co, is being attrited now and will be finished by the end of February.

b) Internal oxidation and reduction - Alloy #3: seven preliminary runs were made with batches of 250 grams of powder in order to choose the best conditions for internally oxidizing the powder, using a fluidized bed technique, described in the last report. The results are given in Table XII.

Table XI

Summary of H_2 Reduction Runs

Run #	Temp. degrees F	Time hrs.	Dew Point of H_2 Gas	Total O_2 w/o	Cr_2O_3 w/o	X-ray Analysis Particle size	X-ray Analysis Peaks	Scanning electron microscope analysis
initial powder	1380	24	-80	0.63	1.2	250 Å	BeO +Cr_2O_3 +$BeCr_2O_4$	much porosity
1	2200	1	-87	0.33	0.21	"	BeO + $BeCr_2O_4$	slight porosity
2	2200	6	-87	0.29	0.21	"	"	complete sintering
3	2200	3	-85	0.42	-	-	BeO +Cr_2O_3 +$BeCr_2O_4$	-
4	2200	13	-80	0.42	-	-	"	-
5	2200	15	-80	0.51	-	-	"	-
6	2200	18	-85	0.57	-	-	"	-
7	1832	12.5	-90	0.50	-	-	"	-
8	2200	16.5	-90	0.25	0.21	-	BeO + $BeCr_2O_4$	-
9	2000	4	-90	0.39	-	-	"	-
10	2200	6	-90	0.30	-	-	"	-
11	2200	24	-90	0.29	-	350Å	"	good sintering particles growth
12	2200	6	-87	0.30	-	-	"	-

Table XII

Summary of Internal Oxidation Conditions

Run #	Alloy	Temp. of Int. Oxid. degrees F	Temp. of Water Bath, degrees F	Gas flow Cu.ft./hr.	Time in hours	Total O_2 wt. %	BeO wt. %	Particle size of BeO*
1	3	1380	150 $\pm$ 1/2	H_2=5 Av.=5	30	0.51	0.78	180 Å
2	"	"	"	"	40	0.58	0.35	-
3	"	"	"	H_2=8 Av.=2	20	0.57	0.42	-
4	"	"	"	"	10	0.60	0.48	-
5	"	1560	"	H_2=10	14	0.63	0.88	200 Å
6	"	"	"	"	20	0.70	-	-
7	"	"	"	"	12	0.73	0.73	-
8	4	"	"	"	6	0.63	-	-
9	"	"	"	"	12	0.69	-	-
10	"	"	"	"	20	0.65	-	300 Å

* BeO particle size is determined by X-ray line broadening after dissolving matrix material

For chemical analysis, after dissolving the matrix, the white residue (BeO) is retained on the filtered paper which is dried, fired at high temperature, and weighed. The particles which are smaller than 100 Å go through the filter paper and are not reported. Thus the BeO contents reported in Table XII are lower than actual. The O_2 analysis is more accurate and should be relied on to find the total conversion time for BeO at a particular temperature. Increasing the internal oxidation time at 1560 degrees F results in a somewhat coarser BeO (see Run #10, Table XII). The O_2 required for converting Be to BeO is between 0.6 - 0.7 weight percent; Table XII shows that between 10 to 20 hours at 1560 degrees F with PH_2O/H_2 ratio 0.3 is sufficient for total conversion to BeO.

Four pounds of #3 alloy have been internally oxidized in batches of 250 grams each, run at 1560 degrees F with a water bath temperature of 150 $\pm$ 1/2 degrees F, which corresponds to a PH_2O ratio of approximately 0.3; with H_2 flow ratio of 10 cubic feet per hour, the powder bed is heat fluidized. The powder tends to cake only slightly; no sintering was observed in any of the runs.

The average particle size of the BeO as determined by X-ray line broadening is between 200 - 250 Å.

The internally oxidized powder was reduced in hydrogen with dew point < -87 degrees F for 12 hours at 1380 degrees F plus 4 hours at 1560 degrees F. After reduction the powder was transferred into 2" I. D. rubber-lined cans (for cold isostatic compaction) in a dry box with argon atmosphere.

The dry box was first evacuated to less than 30 microns and flushed twice with argon and back filled with argon at one atmosphere pressure. After pouring the powder into the lined containers, the cans are vacuum pumped and cold isostatically pressed at 65,000 psi.

Alloy #4: Three preliminary internal oxidation runs were made to standardize the conditions for internally oxidizing this alloy; work is continuing.

3. Ni-Mo-Co-Al-Al_2O_3 Alloys by Surface Oxidation

Following the success with Cu-Al-Al_2O_3 alloys by surface plus internal oxidation of finely attrited flake powders, the process is now being applied to more highly alloyed (solid solution) nickel base alloys to evaluate the potential of the process and the alloys for possible commercialization.

Preliminary experiments indicated that approximately 90 hours of grinding time in the attritor was necessary to reduce -100 mesh inert gas atomized alloy powder into flake-shaped particles with thickness less than 1 micron and an average flake diameter of about 10 microns.

Accordingly, 5 pounds each of the following alloys have been comminuted to the size and shape described above. Note that these alloys are free of chromium, which would have presented major difficulties in subsequent reduction of the Cr_2O_3 formed during attrition. It is hoped that sufficient aluminum will remain to enhance oxidation resistance, at least in alloys 2 and 3.

Alloy	Co	Mo	Al	Ni
		(weight percent)		
Ni-1	20	7	1	bal.
Ni-2	20	7	3	bal.
Ni-3	20	7	6	bal.

Experiments on hydrogen reduction of the comminuted powders have shown that a reduction treatment consisting of holding the powders for 20 hours at 600 degrees C (1112 F) to remove NiO and other oxides of low stability and then shifting the temperature to 925 degrees C (1700 F) and holding for 6 additional hours provides optimal results. This heat treatment serves a threefold purpose:

a) permits removal of excess O_2 from the alloy system
b) permits removal of NiO at a low enough temperature to prevent NiO-Al_2O_3 spinel formation
c) allows the conversion of various low temperature Al_2O_3 crystal forms to the stable hexagonal α Al_2O_3 structure.

In the light of the progress on this alloy system, arrangements are being made for reduction, compaction and consolidation by hot extrusion of these alloy powders. Extrusion will be at 982 degrees C (1800 F) for all alloys. Alloy 1 will be extruded at a ratio of 20:1 while alloys 2 and 3 will be extruded at a ratio of 30:1. It is estimated that consolidated material will be in house and available for testing by the end of March.

4. Copper-Beryllia and Copper-Alumina Alloys Produced by Internal Oxidation of Fine Powders

In the past, the most successful OD alloys were those prepared by internal oxidation (Preston and Grant). Copper, being easy to work with and prepare as OD material, was again chosen to provide adequate material of controlled structure and properties for a number of important physical and mechanical measurements which must be made to advance the state of knowledge regarding OD alloys.

A series of Cu-base alloys in the form of inert gas atomized -325 mesh powders were obtained. These materials have the following compositions (weight percent):

Alloy	Al	Be	Ni	Cu
Cu-1	-	0.5	-	bal.
Cu-2	-	0.8	-	bal.
Cu-3	0.8	-	-	bal.
Cu-4	0.8	-	30	bal.

About 3 pounds of each alloy have been internally oxidized to provide a dispersion of either beryllia or alumina in the Cu or Cu-Ni matrix. A H_2O/H_2 mixture was used to provide the oxygen source.

Alloy 1 has been treated so as to convert all the Be to BeO, while alloy 2 was treated to convert 0.5% Be to BeO; the remaining 0.3 w/o Be will be used as a solid solution strengthener.

Alloys 3 and 4 have been treated so as to convert all the Al in solution to Al_2O_3. These treatments have produced 4 Cu-base alloys with nearly equal volume fractions of dispersoid.

A number of important comparisons can be made, and several points of unknown weight can perhaps be settled from studies of these 4 copper OD alloys; they are:

a) Is BeO a more effective oxide dispersoid than Al_2O_3? BeO does not undergo phase transformations whereas Al_2O_3 can exist in several crystallographic forms.

b) For comparable internal oxidation treatments, will the BeO oxide particles be significantly finer than the Al_2O_3? The heat of formation of BeO is significantly larger (negative) than that for Al_2O_3. Or, in view of the very large difference between the heats of formation of BeO or Al_2O_3 versus CuO, will the resultant particle size be about the same?

c) Is it possible to produce a spinel-free Cu-Al_2O_3 alloy in the presence of as much as 30 percent Ni ($NiO.Al_2O_3$)?

The earlier reported studies by Preston and Grant and Komatsu and Grant with Cu OD alloys will serve as a basis for comparison.

5. Fe-BeO Alloys - Sub-structure Refinement and Electron Microscopy Studies

A study has been initiated with an Fe - 1 v/o BeO alloy and an Fe - 3 v/o BeO alloy, both produced by internal oxidation. The starting condition for these materials is the as-extruded-plus-recrystallized state, produced by holding for 1 hour at 1832 degrees F (1000 C) (in the γ -Fe range) followed by furnace cooling to room temperature. This type of OD alloy is an ideal material for critical studies because of the ease with which one can wipe out the cold worked state by going through the α to γ transformation which occurs at a sufficiently low temperature to avoid any changes in BeO size and distribution.

Preliminary work has revealed the recrystallized material to be completely free of any residual substructure and hence an ideal starting material for further thermomechanical treatment. Bar stock of the alloys has been heat-treated and is ready for use.

The initial work will center around dislocation substructure formation as a function of increasing cold work in the materials. As indicated above, the effect of volume fraction of dispersoid will also be investigated.

The second phase of the work will focus on dislocation substructure rearrangement as a function of annealing treatments. Work done in this laboratory in an earlier NASA study with Fe-BeO materials will serve to provide important background information to correlate dislocation substructure and resulting high temperature creep behavior.

Techniques for producing thin foils of the alloys suitable for study in the electron microscope have been developed, and the program is entering the first phase of the study.

6. Titanium Carbide Dispersion Strengthened Nickel Base Alloys

Using a nickel base alloy (30 Co, 10 Fe, 3 W, 3 Mo, 4 Ti, bal. Ni), experimental alloys of the following types were produced:

Alloy 1: extrusion of the as-received powder

Alloy 2: dry additions of carbon black to the as-received powder

Alloy 3: attrited as-received powder, with dry additions of carbon black, followed by extrusion

Alloy 4: attrited as-received powder, with wet additions of carbon black, followed by extrusion.

Alloy 4 was an attempt to create the optimum carbide dispersion by providing a short diffusion path for the carbon through attrition of the metallic powder to a very fine size and by attemtping to provide an intimate contact of carbon black with the matrix powders by wet blending. The pertinent extrusion conditions are listed below in Table XIII.

Table XIII

Extrusion Conditions

Alloy #	1	2	3	4
Nominal vol. % TiC	Control	4	4	7
Type of carbon black	none	Germantown	Germantown	Sterling MTX-25
Evacuation, time/temperature	12 hr. 500 degrees F	12 hr. 500 degrees F	12 hr. 500 degrees F	12 hr. 600 degrees F
Extrusion pre-treatment	1450 F, 5 hr., heat to 1850 F N_2 atmos.	same as Alloy 1	same as alloy 1	Heat to 1950 F, N_2 atmos.
Extrusion ratio	16:1	16:1	16:1	16:1
Ram speed	200 in/min.	200 in/min.	200 in./min.	140 in/min.
Extrusion post-treat.	Air cool	Air cool	Air cool	Water quench
Initial metallic particle size	20-40 microns	20-40 microns	10-20 microns	7 microns

In the as-attrited condition, alloy 4 contains 2 weight percent oxygen which must be removed by heat treating at 1300 - 1500 degrees F in hydrogen. Unfortunately, air entered the reduction chamber through a leak in a coupling and contaminated the system. In addition, it was found that carbon retarded powder sintering. As chemical analyses show, the above hydrogen treatment did not decrease the oxygen content (see Table XIV).

Table XIV

Results of Chemical Analyses Performed on Carbon Blacks and Alloys 1, 2, 3, and 4

Material	C, wt. %	O, wt. %	Amt. C initially added	Comments
Germantown lamp black	96.1	1.29	-	-
Sterling MTX-25	99.05	0.19	-	-
Alloy 2	-	0.012	0.48	as-extruded; dry mixed Germantown lamp black
Alloy 3	0.47	0.07	0.48	attritted alloy powder: dry mixed Germantown lamp black
Alloy 4	0.59	0.92	1.0	attrited alloy powder: wet additions of MTX-25 carbon
Alloy 4	0.48	1.50	1.0	As-extruded

The oxygen contained in the Germantown lamp black (Table XIV) accounts for 3/4 of the total oxygen in alloy 2, and less than 1/2 in alloy 3. Surface oxygen makes up the difference in alloy 2 while the additional oxygen in alloy 3 must come from the attrition operation.

Two possibilities account for the loss of carbon in alloy 4 from the initial amount added: separation in the blender, and reaction with air and hydrogen in the furnace. Regardless of the exact cause of carbon depletion, more than 1/2 of the initial carbon content was lost in the preparation of alloy 4, and an excess amount of oxygen was introduced.

The microstructural constituents of alloy 4 were estimated in the following manner: from the free energies of formation of possible oxides and carbides that could be found in alloy 4, it was assumed that oxygen reacts preferentially with Ti to form TiO_2, then with W, and finally with Mo. Carbon reacts preferentially with Ti, then W, and finally Mo. Based on 1.5 percent oxygen and 0.48 percent C, 3.7 weight percent TiO_2, 1.84 percent TiC, and 0.59 percent WC would be present, adding up to 11.1 volume percent of dispersoid. An electron microprobe study on alloy 3 indicated that TiC formed with no interference from Mo and W; thus all the C probably formed TiC in alloy 4 before WC could form.

Room temperature strength properties: Alloys utilizing carbide dispersed phase strengthening will have higher yield and ultimate tensile strengths than solid solution alloys if the amount of dispersoid is not excessive. For incoherently dispersed phase systems, a high dislocation density strengthens these materials. For coherently dispersed phase systems, both internal lattice strains and a high dislocation density are the strengthening mechanisms. Too much dispersed phase or too much coarsening of the particles during high temperature exposure will result in embrittlement or low strength values, respectively. The low ultimate tensile strengths of alloys 2, 3, and 4, from 145,000 to 125,000 psi (see Table XV), yield strengths no greater than the yield strength of the control sample (96,000 psi), and the relatively high ductility values suggest that the samples did not fully retain the cold work of extrusion which was expected. The Murphy alloy gave a yield strength near 140,000 psi, seven times that of his matrix control alloy, in the as-extruded condition, as against 96 to 97,000 psi reached here.

Figure 11 is a plot of log stress versus log rupture time for tests at 1600 and 1800 degrees F, and includes the 1800 degree F values for the best previous Ni-TiC alloy reported by Murphy and Grant. Of importance are the following:

a) The more complex and solid solution, nickel base alloys, dispersion strengthened with TiC, are significantly stronger than the simple Ni-TiC alloy (Murphy and Grant).

b) In view of the improved room temperature properties, the observed 1800 degree F properties for these alloys are interesting and promise further important improvements.

c) In progressing from alloys 1 to 4, not only are the 1800 degree F properties higher, but the stability is improved in an important way, as measured by the increasingly flat slope of the alloys in the progression.

Table XV

Results of Mechanical Testing

Alloy	1	2	3	4	Internally carburized Ni-TiC*
As-extruded Rockwell C hardness	23	27	21	27	-
Y.S.(0.2%) at 70 degrees F, psi	96,000	95,000	78,750	97,500	broke at 162,000 psi in threads without yielding
U.T.S. at 70 degrees F, psi	160,000	145,000	132,000	125,000	
Elongation, %, at 70 degrees F	41	34	25	12.5	
Reduction in area, %, at 70 degrees F	55	35	13	9	-
Recrystallization or softening temperature, degrees F	1500	1600	-	1300 to 1400	-
Stress for 50 hour life at 1800 degrees F, psi	2500	3700	4600	5600	2700
Stress for 100 hour life at 1800 degrees F, psi	2200	3200	4200	5000	2400
Fracture	ductile	ductile	ductile/ brittle	brittle	brittle
Volume % TiC	0	3.6	3.6	11.1	15.4

* From the work of Murphy and Grant

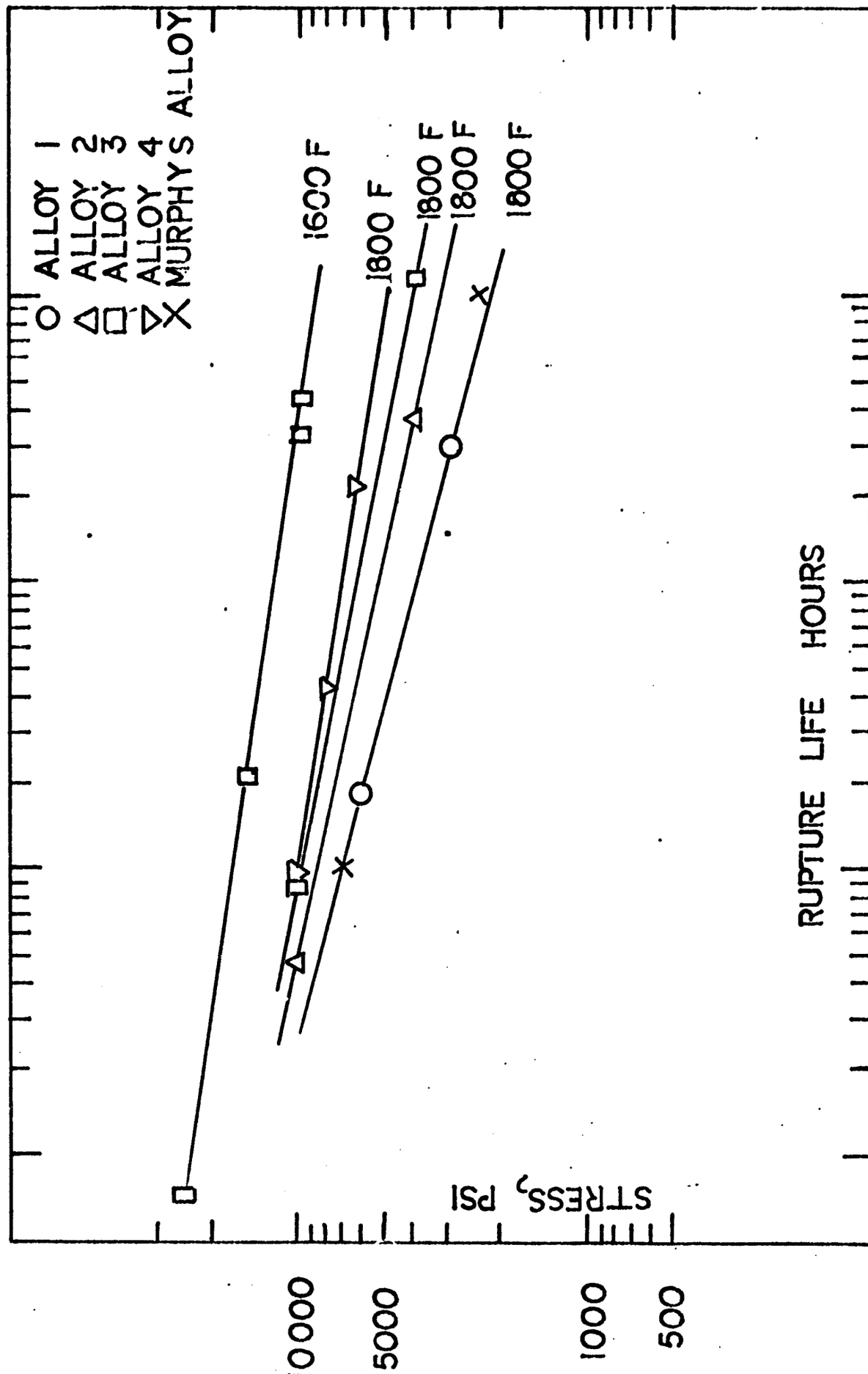

Figure 11. Hardness at room temperature versus 1 hour annealing for alloys 1 and 2

Figure 12, minimum creep rate versus reciprocal temperature, yields activation energies for creep of these alloys. The number of points is unfortunately too small for accurate determination of values, nevertheless values of -117,000 cal per g. atom for alloy 3, and values of -81,000 and -97,000 for alloy 4 compare with -65,800 for the self diffusion value for pure nickel, indicating a more stable, more creep resistant structure for the TiC strengthened nickel alloy structures.

Of particular interest are the structure stability patterns exhibited by these alloys. TiC is soluble in nickel base alloys, leading to softening and weakening at relatively low temperatures compared to OD Ni base alloys, in which the oxide is insoluble. Figure 13 compares the room temperature hardness after 1 hour exposures at progressively higher annealing temperature for alloys 1 (control) and 2 after 60 percent cold reduction. Alloy 1 softens normally, progressively from about 400 degrees F; alloy 2 maintains its hardness to about 1200 degrees F before annealing rapidly at higher temperatures. The relatively small amount of TiC in alloy 2 is only a temporary stabilizer of structure.

Figure 14 shows a similar plot for alloy 4, the strongest alloy with the highest content of TiC. The decrease of hardness for the as-extruded alloy on exposure to 1800 degrees F is small, indicating excellent stability. Cold reduction of the as-extruded product raises the room temperature hardness significantly; even though this high hardness is not fully maintained, the hardness at 1800 degrees F is still quite high, finally falling to the same values as the as-extruded material at 2000 to 2200 degrees F. Thus the 11.4 volume percent of TiC in this nickel base alloy is an effective deterent to recrystallization, and, considering the early state of these alloys, is an effective room temperature strengthener and high temperature strengthener to at least 1800 degrees F.

Future Work

Experiments with an electron microprobe will determine the components of the bulky precipitate found in alloy 4 which, in turn, will furnish information on this system's chemistry.

Creep tests are in progress on chromium plated specimens of alloy 4 to ascertain the extent of the oxidation problem and the ability of the structure to retain the internal strain energy of cold work.

Two new alloys are also planned. In the first alloy, TiC will form from the decomposition reaction of Fe_3C that will be blended with the matrix powders. This is an effort to produce a much finer, more uniform TiC dispersion. In the second alloy, a dual Al_2O_3-TiC dispersion will strengthen the alloy while free aluminum in the matrix should improve oxidation resistance. Here, the TiC will be added to the matrix as 0.1 micron powder and the Al_2O_3 will be produced during the attrition of -100 mesh matrix to 10 micron flakes.

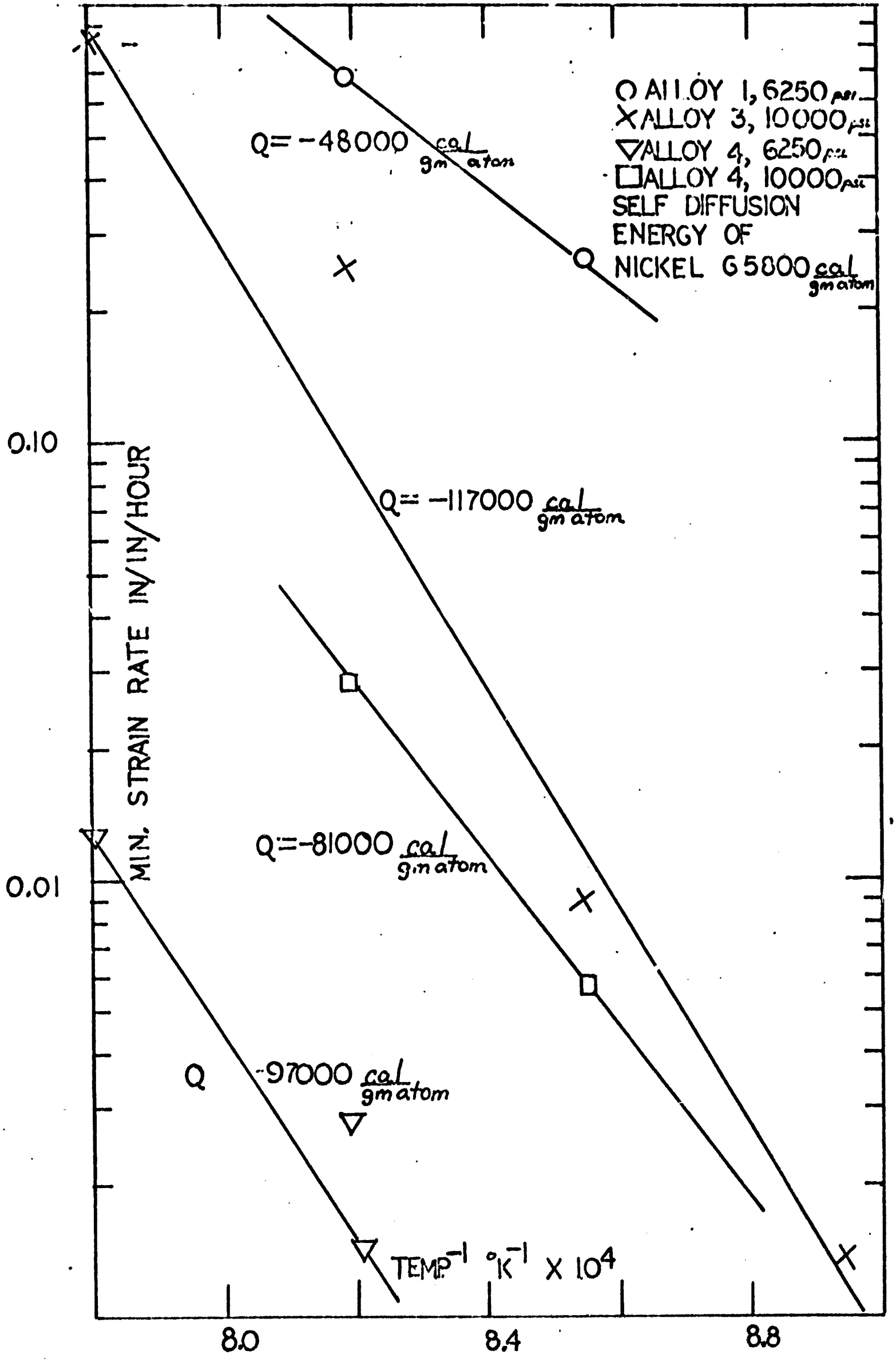

Figure 12. Activation energy calculated from minimum creep rate versus reciprocal temperature measurements

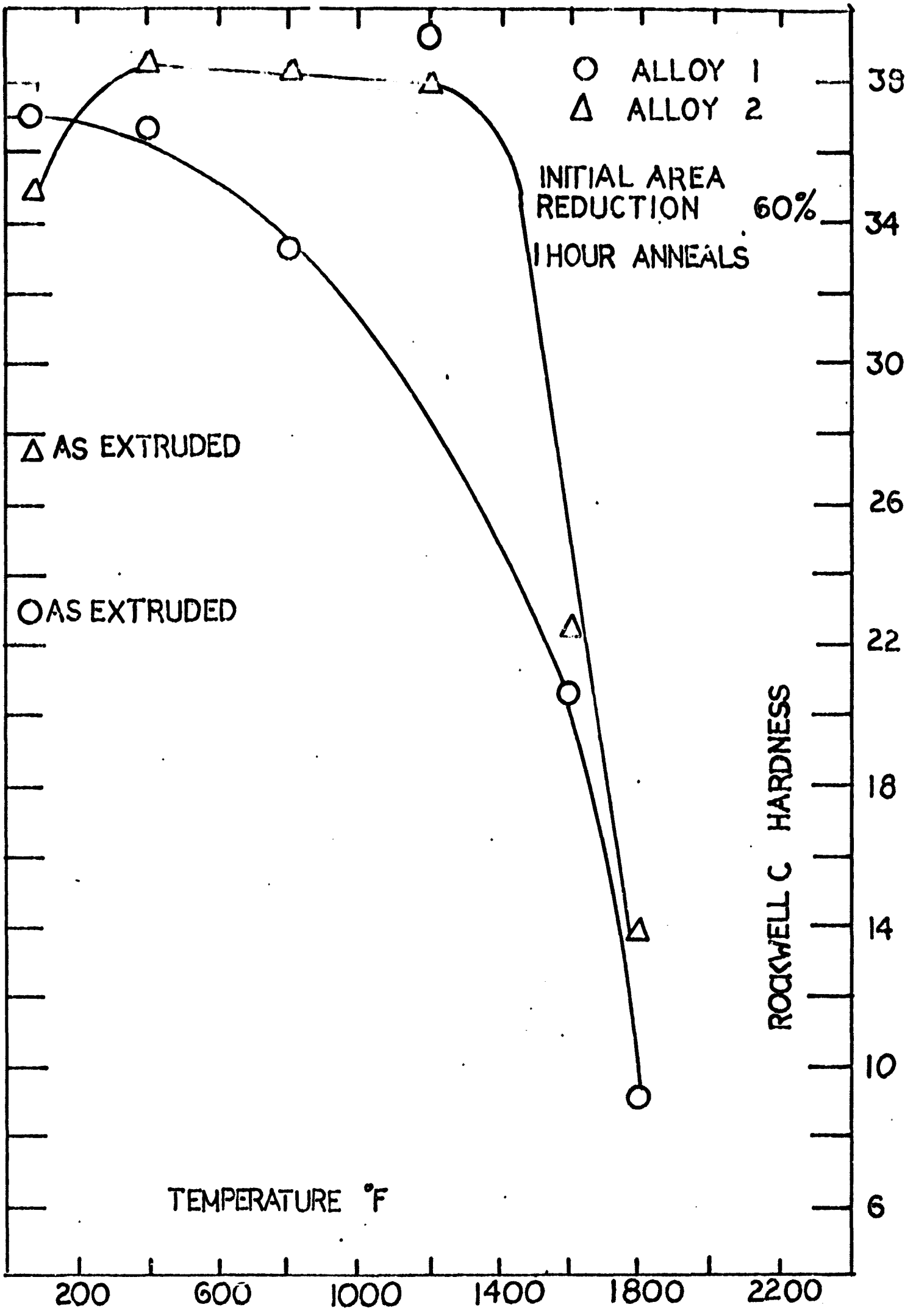

Figure 13. Log stress versus log rupture time for TiC dispersion strengthened nickel base alloy

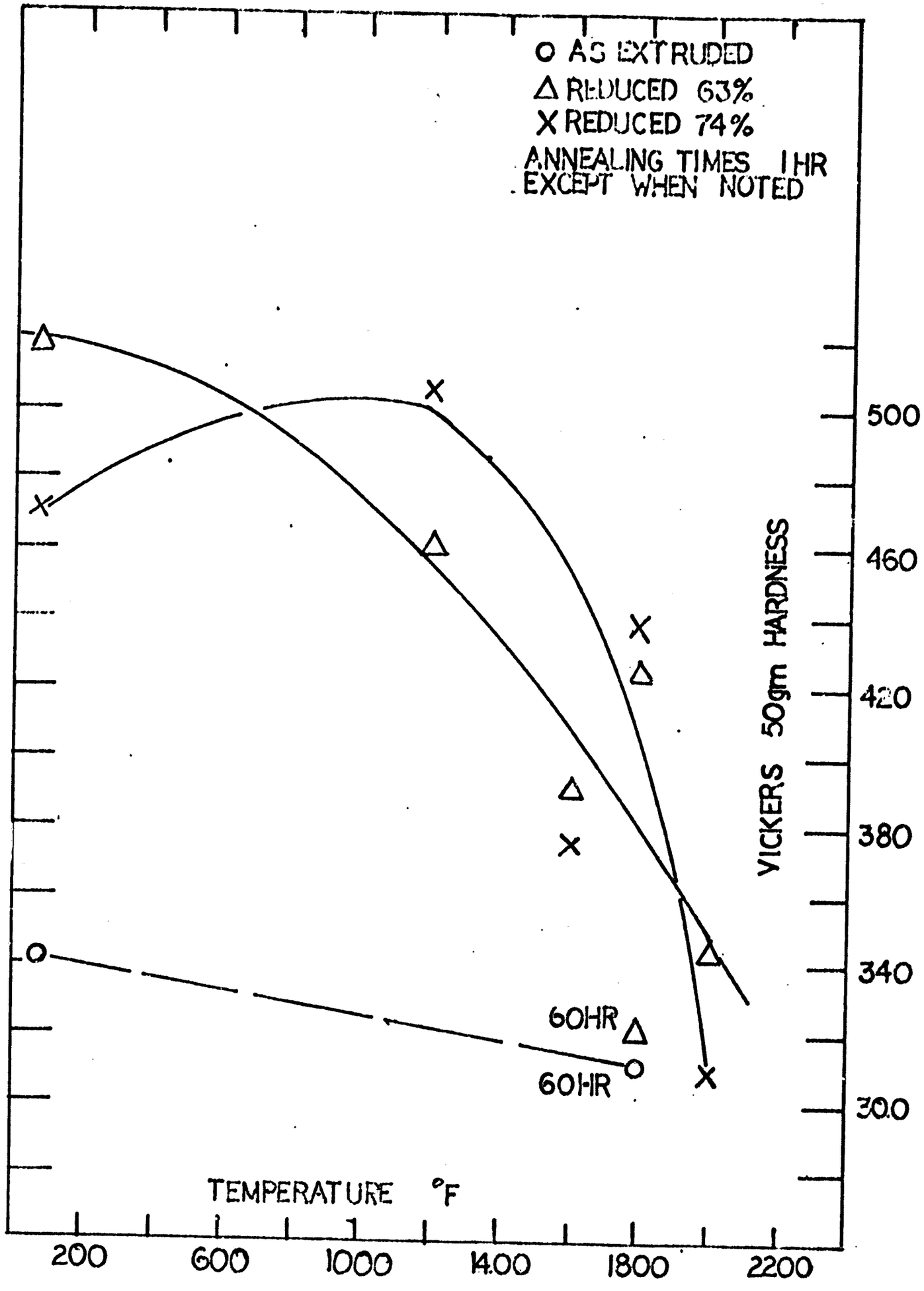

Figure 14. Room temperature hardness versus 1 hour annealing time

II. CONTROL OF STRUCTURE AND PROPERTIES BY MEANS OF RAPID QUENCHING OF LIQUID METALS (SPLAT COOLING)

7. Splat Cooling of Aluminum Alloys

Aluminum-Silicon Alloys - Considerable difficulty was experienced in splat cooling the aluminum-silicon alloys against a stainless steel wheel. Unlike 2024 aluminum, the aluminum-silicon alloys adhered strongly to the steel wheel upon solidification. Many attempts at using various blades and blade configurations and scraping systems were all unsuccessful at removing the aluminum-silicon flakes in a continuous manner. Flake build-up destroyed the quenching effect of the steel wheel, cancelling out its effectiveness. Following trials with different materials, a copper disc 14 inch in diameter and 1/2 inch thick was machined and used as the splat wheel. Successful splat runs have been made on this wheel with both an Al-7.4 weight percent Si alloy and the control 2024 alloy. The aluminum-silicon alloys do not stick to the copper wheel and can be readily removed by the steel doctor blades.

Work is now progressing as rapidly as possible to produce an Al-7.4 weight percent Si alloy and a 2024 aluminum splat cooled alloy. Both alloys will then be cold compacted in aluminum cans, evacuated briefly at 490 degrees C to remove water of hydration ($Al_2O_3 . 3H_2O$) and extruded at 300 degrees C at an extrusion ratio of 20:1.

Extruded Air Atomized Alloys - Two new extrusions of a coarse, air atomized Al-7 weight percent Si alloy and a 2024 alloy have been produced. Both materials were cold compacted at 20,000 psi into aluminum cans, evacuated at 300 degrees C, and extruded at 300 degrees C at a 20:1 extrusion ratio.

This second air atomized 2024 powder extrusion was made with a larger final core diameter (.9 inch) in order to permit refining of the retained coarse particle boundaries, which are elongated parallel to the extrusion direction. While the dendrite and grain size are of desired dimensions, the powder particle boundaries are preserved after a 10 to 1 or 20 to 1 extrusion ratio, leading to undesirable determinations. By alternate steps of swaging to 25 percent reduction in area and annealing above the recrystallization temperature, a much finer structure should be produced, and the powder particle boundaries will be completely broken up. Preliminary work on swaging and annealing the previous 2024 air atomized extrusion has shown that the total structure can indeed be refined by this process.

At present this second 2024 extruded alloy is being processed with the expectation of significant further improvements in the tensile and fatigue properties and in the fracture behavior.

Room temperature tensile tests were run on the air atomized Al-7 weight percent Si alloy in the as-extruded condition. The tests were performed on an Instron machine at a cross-head speed of .05 inch/minute. Standard 1/4 inch diameter by 1 inch gauge length tensile specimens were used. The excellent results are given below in Table XVI and are compared with commercial high silicon casting alloys.

Table XVI

Room Temperature Tension Test Results

Alloy	Condition	0.2% Y.S., psi	U.T.S., psi	Elong.,%	R.A.,%
Al -7% Si	air atomized alloy, as-extruded	17,350 17,200	27,600 27,600	25 27	39 42
Alloy 43 (5% Si)	die cast sand cast perm. mold cast	16,000 8,000 9,000	33,000 19.000 23,000	9 8 10	- - -
Alloy 356*	sand cast, T-6 sand cast, T51 perm. mold, T-6	24,000 20,000 27,000	33,000 25,000 38,000	3.5 2 5	- - -

* 7% Si, 0.3 Mg

Note the excellent strength and very high ductility of the air atomized Al-7% Si in the as-extruded condition. This alloy is not heat treatable, whereas alloy 356 is; accordingly, comparisons should be made with alloy 43 instead. Further refinement of structure of the Al-7% Si alloy by splat cooling should enhance the properties even more.

The increased strength and ductility in the extruded, air-atomized alloy is due to the much finer size and distribution of the silicon particles in the aluminum matrix. The large silicon particles (15 microns long and 2 microns wide) present in conventionally cast ingots have been refined to about 2 microns in the extruded, air-atomized material.

Future Work

In the next six months the following program is planned. Two new extrusions of an Al-7.4 weight percent Si and a 2024 alloy, as splat cooled products, will be processed identically to the air-atomized extrusions. The extruded 2024

splat cooled material will be alternately swaged and annealed in a like manner to the 2024 air-atomized material. The two materials will then be tested in tension and fatigue and compared with commercial 2024-T4 aluminum. By measuring the volume fraction, average particle size, and interparticle spacing of the intermetallic inclusions in each of the three alloys, a good correlation among cooling rate, particle size and distribution, and mechanical behavior in tension and fatigue should be established.

The air-atomized and splat cooled aluminum-silicon alloys will be compared in tension and creep-rupture tests. Again, the size and distribution of the silicon particles in the aluminum matrix will be correlated with the mechanical properties of the two alloys. The splat material with its finer silicon size and distribution should give higher strength and creep resistance than the air atomized material.

8. Increased Terminal Supersaturation in Al-Cu, Al-Fe, and Al-Si by Splat Cooling

Equipment Modifications - The high temperature, inert gas atmosphere, splat machine has been modified to allow several splats to be made (without opening the apparatus). A vacuum valve and evacuation port in the shock tube permits loading specimens and insertion of new diaphragms without the necessity of cooling the furnace and re-evacuating the splat chamber for each splat. Thus, at least three times as much splat material can be produced in the same amount of time.

Decomposition Studies - X-ray studies of the decomposition from supersaturated solid solution of Al-Fe and Al-Cu are continuing. Lattice parameter versus composition curves for Al-4% Fe (at 250 degrees C) and Al - 4% Cu (at 300 degrees C) have been completed. Similar measurements for higher annealing temperatures for Al-Fe are in progress.

Calculations have been made to show that the anomolously large amount of X-ray line broadening observed from splat cooled foils may be produced by composition variation in the foils. Several possible composition profiles were assumed; the diffraction peaks which would result from each assumed composition distribution were then calculated. A diffraction peak (for Al-10% Si) was calculated, assuming equal amounts of material of all compositions between that of pure Al and a completely supersaturated Al-10% Si alloy very closely matched the observed diffraction peaks for this system. Therefore, it is likely

that the broadening seen in the Al-Si system is almost entirely due to composition variations. This is further supported by the fact that this explanation could also account for the asymmetric peak shapes often seen for this system and the variable diffraction peak location for different splits made from the same alloy. That the broadening is due to composition variation is strongly supported by the observation that transmission electron micrographs of Al-Si alloys show precipitated regions even in foils with the maximum amount of supersaturation, as measured by lattice parameter shift.

Scanning Electron Microscopy - Splat cooled foils of Al-Fe and Al-Cu have been examined by scanning electron microscopy. As was expected, the surface of the splat which was in contact with the substrate appears to be a negative of the substrate. The intimate contact between the substrate and the splat is shown by the fact that the microscopic scratches left on the substrate during polishing are faithfully reproduced on the splat surface. The large numbers of extremely irregularly shaped holes is the other striking feature of these foils when seen from the underside. From this observation, it is readily understandable that a substantial percentage of the splat foil area is sufficiently thin in the as-splatted condition for direct observation by transmission electron microscopy.

The upper surfaces of the splat foils are extremely irregular. That the foils are composed of layers of flattened droplets is clearly observable. A substantial number of spherical droplets as well as partially flattened droplets are found on the upper surface. These prematurely frozen droplets are a useful indicator of the molten droplet size. Previous measurements in this, laboratory established a droplet size of from 1 to 50 microns in diameter with a 3 micron diameter the most commonly observed size. The sizes were measured from high-speed silhouette photographs taken just prior to impact. Sizes measured from the scanning electron micrographs are consistent with these measurements. Most of the droplets measured ranged in size from 1 to 10 microns with many droplets around 3 micron in diameter.

Al-Cu splats of different compositions (4 to 9 atomic percent Cu) were compared and no differences in external appearance were observed. Splats of Al-Fe appear very similar to Al-Cu splats, but are somewhat more irregular. Al-Cu splats made in air were also examined for comparison with Al-Cu splats made in an inert gas atmosphere. The upper surfaces differ substantially. The foils made in air have a very cellular appearance, in addition, many fewer spherical droplets are found.